Dual 5-HT 6 and D 3 Receptor Antagonists in a Group of 1 H -Pyrrolo[3,2- c]quinolines with Neuroprotective and Procognitive Activity

Katarzyna Grychowska, Séverine Chaumont-Dubel, Rafal Kurczab, Paulina Koczurkiewicz, Caroline Deville, Martyna Krawczyk, Wojciech Pietruś, Grzegorz Satala, Kamil Piska, Marcin Drop, et al.

Dual 5-HT$_6$ and D$_3$ Receptors Antagonists in a Group of 1*H*-Pyrrolo[3,2-*c*]quinolines with Neuroprotective and Pro-cognitive Activity

Katarzyna Grychowska,[a] Severine Chaumont-Dubel,[b] Rafał Kurczab,[c] Paulina Koczurkiewicz,[d] Caroline Deville,[a] Martyna Krawczyk,[e] Wojciech Pietruś,[c] Grzegorz Satała,[c] Kamil Piska,[d] Marcin Drop,[a] Xavier Bantreil,[f] Frédéric Lamaty,[f] Elżbieta Pękala,[d] Andrzej J. Bojarski,[c] Piotr Popik,[e] Philippe Marin,[b] Paweł Zajdel[a,*]

[a] *Department of Medicinal Chemistry, and* [d] *Department of Pharmaceutical Biochemistry Jagiellonian University Medical College, 9 Medyczna Str., 30-688 Kraków, Poland*

[c] *Department of Medicinal Chemistry,* [e]*Department of Behavioral Neuroscience and Drug Development, Institute of Pharmacology, Polish Academy of Sciences, 12 Smętna Str., 31-343 Kraków, Poland*

[b] *IGF, Université de Montpellier, CNRS INSERM, Montpellier, France*

[f] *IBMM, UMR 5247, CNRS, Université de Montpellier, ENSCM, Place Eugène Bataillon, 34095 Montpellier, France*

*Corresponding author:
Paweł Zajdel
Department of Medicinal Chemistry
Jagiellonian University Medical College
E-mail: pawel.zajdel@uj.edu.pl
Tel.: +48 126205450

Abstract

In light of the multifactorial origin of neurodegenerative disorders and some body of evidence indicating that pharmacological blockade of serotonin 5-HT_6 and dopamine D_3 receptors might be beneficial for cognitive decline, we envisioned (*S*)-1-[(3-chlorophenyl)sulfonyl]-4-(pyrrolidine-3-yl-amino)-1*H*-pyrrolo[3,2-*c*]quinoline (CPPQ), a neutral antagonist of 5-HT_6R, as a chemical template for designing dual antagonists of 5-HT_6/D_3 receptors. As shown by *in vitro* experiments, supported by quantum chemical calculations and molecular dynamic simulations, introducing alkyl substituents at the pyrrolidine nitrogen of CPPQ, fulfilled structural requirements for simultaneous modulation of 5-HT_6 and D_3 receptors.

The study identified compound **19** ((*S*)-1-((3-chlorophenyl)sulfonyl)-*N*-(1-isobutylpyrrolidin-3-yl)-1*H*-pyrrolo[3,2-*c*]quinolin-4-amine), which was classified as a dual 5-HT_6/D_3Rs antagonist ($K_{i\ (5\text{-}HT6)}$ = 27 nM, $K_{i\ (D3)}$ = 30 nM). Compound **19** behaved as a neutral antagonist at G_s signaling and had no influence on receptor-operated, cyclin-dependent kinase 5 (Cdk-5)-dependent neurite growth. In contrast to the well characterized 5-HT_6R antagonist intepirdine, compound **19** displayed neuroprotective properties against astrocyte damage induced by doxorubicine, as shown using 3-(4,5-dimethylthiazol-2-yl)-2,5-diphenyltetrazolium (MTT) staining to assess cell metabolic activity and lactate dehydrogenase (LDH) release as an index of cell membrane disruption. This feature is of particular importance considering the involvement of loss of homeostatic function of glial cells in the progress of neurodegeneration. Biological results obtained for **19** in *in vitro* tests, translated into pro-cognitive properties in phencyclidine (PCP)-induced memory decline in the novel object recognition (NOR) task in rats.

Key words:

5-HT_6R antagonists, D_3R antagonists, Cdk5 signaling pathway, multifunctional ligands, salt bridge, molecular dynamics, neuroprotection, astrocytes, novel object recognition test

Introduction

Cognitive impairment is a common feature of neurodegenerative and psychiatric diseases. This type of decline involves a variety of cognitive domains, including memory, attention, language comprehension and problem-solving skills.[1] Deficits in these functions contribute to a poor level of social interaction and decreased quality of life. Although various procognitive drug candidates have been investigated in clinical trials for cognitive dysfunctions in Alzheimer's disease (AD) and schizophrenia, no disease modifying treatment has been clinically validated so far. Thus, development of new compounds for symptomatic pharmacotherapy still seems to be a valid strategy.

Because of the multifactorial etiology of neurodegenerative and psychiatric disorders, selective drugs have shown limited efficacy in clinical trials.[2,3] One example is represented by serotonin 5-HT_6R antagonists, which have been widely explored as potential therapy for memory decline in AD. According to recent clinical reports, the positive effects of idalopirdine and intepirdine on memory deficits have not been confirmed in phase III clinical trials. Nevertheless, the exact cause of these results remain unclear and 5-HT_6R antagonism is still being investigated in both preclinical and clinical studies.[4–6]

The constant interest in 5-HT_6R ligands results from the unique properties of this protein. The 5-HT_6R belongs to the G-protein coupled receptors (GPCRs) family and displays high level of constitutive activity at G_s signaling. It also engages additional signaling pathways, such as extracellular kinase 1/2 (ERK1/2)[7] and cyclin dependent kinase 5 (Cdk5), the latter being involved in neurogenesis process.[8,9] 5-HT_6R also recruits several proteins of the mechanistic Target Of Rapamycin (mTOR) pathway which accounts for the impact of the receptor in some cognition paradigms in rodents(Figure 1).[10,11] An additional particular feature of the 5-HT_6R is its exclusive localization in the central nervous system, especially in brain regions involved in learning and memory processes including the prefrontal cortex, hippocampus and stratium.[12,13] Because 5-HT_6R blockade enhances cholinergic, glutamatergic and noradrenergic transmission, this mechanism has been involved in the improvement of cognitive performance induced by 5-HT_6R antagonists (Figure 1).[14–17]

Another molecular target, which has emerged as promising for developing novel pro-cognitive drugs, is dopamine D_3R. This GPCR is localized in the limbic areas of the brain. In addition to coupling to $G_{i/0}$ protein, it engages other transduction pathways, including Cdk5[18] and mTOR pathways.[19] An additional value of this mechanism of action is the possibility of

enhancing the acetylcholine and glutamate signalling.[20,21] Therefore, blockade of D_3R may improve cognitive decline and also relieve the negative symptoms of psychosis (Figure 1).[22]

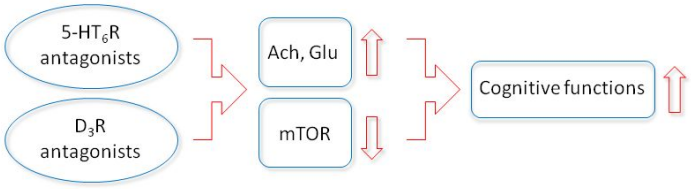

Figure 1. Schematic representation of the hypothetical influence of dual 5-HT_6/D_3Rs antagonists on cognitive functions.

Because cognitive decline is a common symptom of CNS diseases characterized by a loss of neuronal cells, neuroprotective properties may be a valuable add-on effect of pharmacotherapy. Among glial cells, astrocytes play a crucial role in the viability and physiological function of neurons by maintaining proper function of the CNS microenviroment.[23] Astrocytes supply neurons with vital metabolites, initiate cell repair systems and release cytokines and growth factors that exert multidirectional effects. The supporting role of astrocytes in the CNS confers them with intrinsic neuroprotective properties.[24]

The aforementioned observation provided the impetus to design dual 5-HT_6/D_3Rs antagonists that display neuroprotective properties in cellular assays and ameliorate cognitive decline in animal models. Hence, we envisioned introducing various alkyl chains at the nitrogen atom of pyrrolidine in the CPPQ (a neutral 5-HT_6R antagonist with pro-cognitive properties) scaffold (Figure 2).[25] This approach involved the idea of merged ligands, in which alkyl chains, representing pharmacophore fragment of D_3R antagonists, were combined with 5-HT_6R antagonist template.

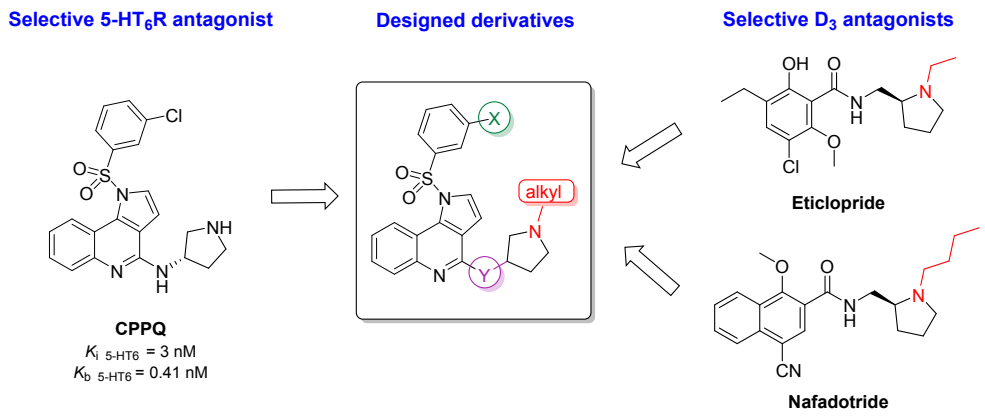

Figure 2. A strategy for designing dually acting 5-HT_6/D_3Rs antagonists.

In accordance to our previous work,[25] chlorine atom in the *meta* position of arylsulfonyl fragment was the most favorable substituent for interaction with the 5-HT_6R. Thus, in order to evaluate the impact of applied modifications on affinity for both receptors, investigations were limited to this substitution pattern. The choice also resulted from preferential role of chlorine atom in stabilization of the ligand-receptor complex by the halogen bonding.[26–28] Finally, to investigate the stereochemical preference of designed derivatives, four pairs of enantiomers were tested. The influence of applied modifications on 5-HT_6/D_3Rs affinity was first tested in *in vitro* studies, supported by *in silico* analysis. The most promising compound **19** was further examined for its functional properties in 5-HT_6R-operated constitutive activity at G_s and Cdk5 signaling and D_3R-operated cAMP signaling. Compound **19** and its active comparators – CPPQ and intepirdine, were subsequently evaluated for their neuroprotective properties in astrocyte cells. Finally, to confirm the presented concept, the ability of **19** to reverse drug-induced memory deficits was measured in the NOR test in rats.

Chemistry

The designed compounds were synthesized using a multistep procedure (Scheme 1), starting from pyrroline **1** obtained following a flow-chemistry approach.[29]

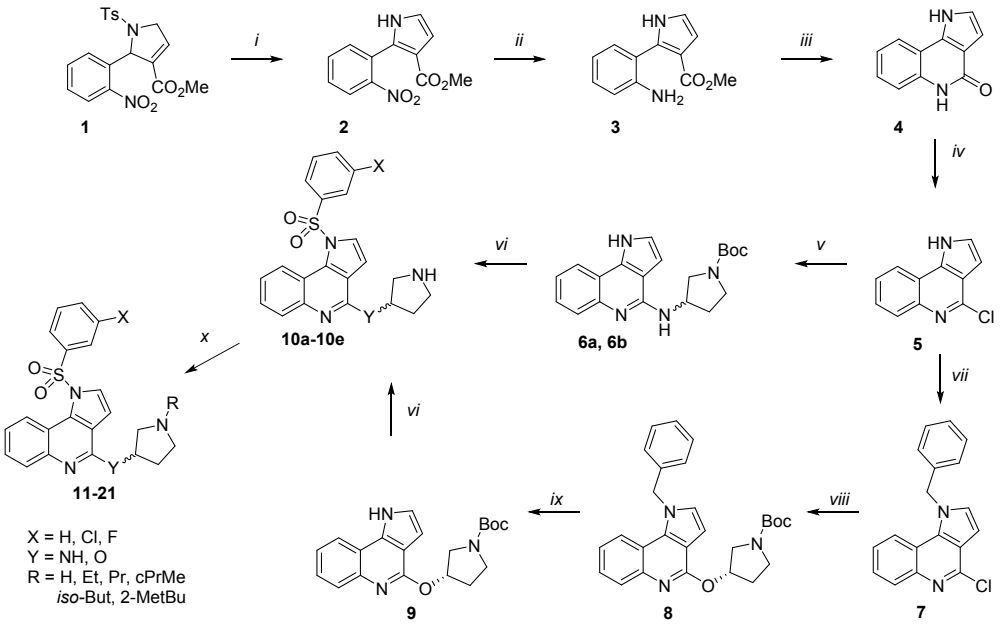

Scheme 1. Reagents and conditions: (*i*) NaO*t*-Bu, DMF, RT, 2 h; (*ii*) H_2, Pd/C, MeOH, RT, 2 h; (*iii*) AcOH, *sec*-BuOH, 60°C, 3 h; (*iv*) $POCl_3$, 105°C, 4 h; (*v*) (*R*)-3-amino-1-Boc-pyrrolidine or (*S*)-3-amino-1-Boc-pyrrolidine, MeCN, MW 140°C, 7h (*vi*) 1. arylsulfonyl chloride, BTPP, DCM, 0°C – RT, 3 h, 2. 1M HCl/MeOH RT, 5h; (*vii*) benzyl bromide, Cs_2CO_3, DMF, RT, 30 min; (*viii*) (*S*)-3-hydroxy-1-Boc-pyrrolidine, $Pd_2(dba)_3$, BINAP, KO*t*-Bu, toluene; MW 114°C. (*ix*) O_2, KO*t*-Bu, DMSO, 70°C, 1h; (*x*) aldehyde, $NaBH_3CN$, EtOH, RT, 12 h.

Removal of the tosyl group in basic conditions (NaO*t*-Bu) allowed for simultaneous aromatization of the pyrroline moiety and generation of pyrrole derivative **2**, which was further reduced using palladium on charcoal under hydrogen atmosphere to yield amino derivative **3**. Heating of the latter with acetic acid in boiling *sec*-butanol allowed intramolecular cyclization to afford lactam derivative **4**, which was submitted for the oxidative chlorination to yield 1*H*-pyrrolo[3,2-*c*]quinoline **5**. Treatment of the synthon **5** with pure enantiomers of 3-amino-1-Boc-pyrrolidine in acetonitrile at 140°C, under microwave assisted conditions, yielded amine derivatives **6a** and **6b**. On the other hand, reaction with (*S*)-3-hydroxypyrrolidine, required prior introduction of benzyl protecting group at the *N*1 position of pyrroloquinoline to obtain derivative **7**. This route enabled O-arylation with a Boc-protected aminoalcohol under Buchwald-Hartwig conditions, yielding compound **8**. The benzyl group in **8** was subsequently removed by bubbling compressed air into a DMSO solution of **8**, in the presence of KO*t*-Bu at 70°C for 1 h yielding **9**.[30] Coupling of compounds **6a**, **6b** and **9** with selected arylsulfonyl chlorides in the presence of a phosphazene base, P1-*t*-Bu-tris(tetramethylene) (BTPP), provided arylsulfonyl derivatives of Boc-protected *N*-4-(pyrrolidin-3-ylamino)-1*H*-pyrrolo[3,2-*c*]quinolines (**10a**–**d**) and *O*-4-(pyrrolidin-3-ylamino)-1*H*-pyrrolo[3,2-*c*]quinoline (**10e**). Subsequent removal of the Boc group in acidic conditions furnished hydrochloride salts of the secondary amines. The obtained derivatives **10a**–**10e** were further submitted to reductive amination using sodium cyanoborohydride in ethanol at room temperature, yielding final tertiary amines **11**–**21**.

Results and discussion

Pharmacological *in vitro* evaluation and structure-activity relationship studies

Multifunctional drugs, combining several pharmacological effects in a single molecule, constitute a promising strategy for the treatment of multifactorial neurodegenerative and psychiatric diseases. Compounds reported in literature, which simultaneously bind to 5-HT_6 and D_3Rs, display neither high affinity for both targets[31] nor show activity in functional assays.[32,33] In the present study, compound CPPQ, a neutral 5-HT_6R antagonist, was structurally modified with various alkyl substituents at nitrogen atom of pyrrolidine, in order to obtain dual 5-HT_6/D_3Rs ligands (Figure 2).

Synthesized compounds **11**–**21** displayed moderate-to-high affinity for the 5-HT_6R (K_i = 4–106 nM) in [^{3}H]-LSD binding assay. Derivatives selected on the basis of high 5-HT_6R affinity, (K_i values below 30 nM), showed moderate-to-high affinity for D_3R expressed as % inhibition of [^{3}H]-methylspiperone specific binding (77 – 98 % at 1 μM) (Table 1).

Table 1. Binding data of compounds **11**–**21** for 5-HT_6 and D_3 receptors.

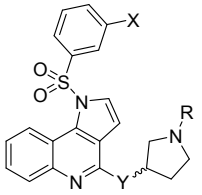

Compd	X	Y	R	R Volume [cm^3/mol]	*R/S*	K_i [nM][a]	%inh binding @ 1μM[b]
						5-HT_6	**D_3**
CPPQ	3-Cl	NH	H	–	*S*	3[c]	69
11	3-Cl	NH	Et	44.471	*R*	52	NT
12	3-Cl	NH	Et	44.471	*S*	11	77
13	3-Cl	NH	Pr	54.052	*R*	61	NT
14	3-Cl	NH	Pr	54.052	*S*	17	87
15	3-Cl	O	Pr	54.052	*S*	21	80
16	3-Cl	NH	*c*PrMe	92.791	*R*	106	NT
17	3-Cl	NH	*c*PrMe	92.791	*S*	41	NT
18	3-Cl	NH	*iso*Bu	59.21	*R*	56	NT
19	3-Cl	NH	*iso*Bu	59.21	*S*	27	98
20	3-Cl	NH	2-MetBu	87.144	*S*	30	78
21	H	NH	Pr	54.052	*S*	51	NT

[a]Mean K_i values, based on three independent binding experiments (SEM ≤ 18%)
[b]Percentage displacement values at 10^{-6} M; performed at Eurofins (www. eurofinsdiscoveryservices.com)
[c]Data taken from ref. [25]

These observations were consistent with results of *in silico* experiments, indicating that generally all obtained compounds (**11**–**21**) show coherent binding modes to the 5-HT_6R. The protonated pyrrolidine moiety formed a salt bridge with D3.32, the 1*H*-pyrrolo[3,2-*c*]quinoline ring formed CH–π interaction with F6.52, and the terminal 3-substituted phenyl ring expanded into a hydrophobic cavity between transmembrane domains (TMs) 3–5 and the extracellular loop 2 (ECL2) (Figure 3A).

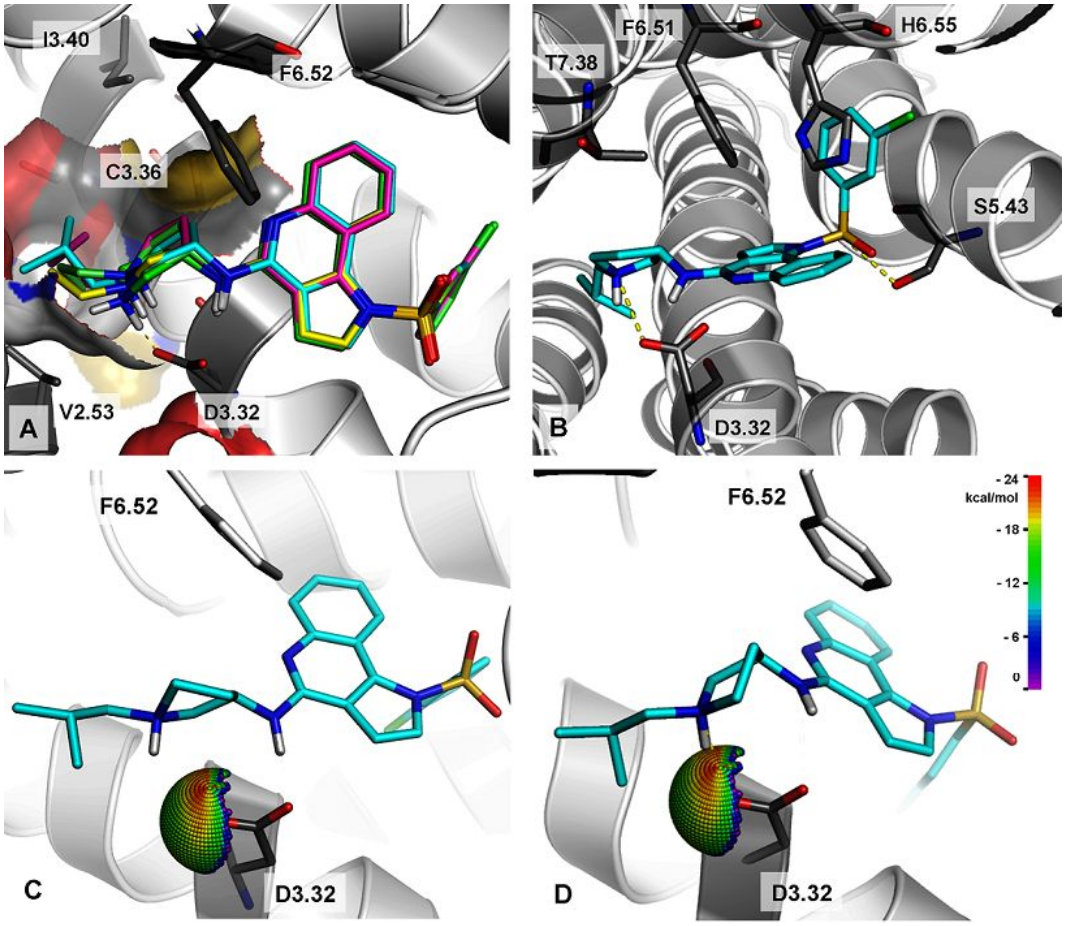

Figure 3. (A) Superposition of the binding mode of *S* enantiomers with different alkyl chains on the nitrogen atom of pyrrolidine in the 5-HT_6 receptor binding site (CPPQ–green, **12**–yellow, **14**–lime, **17**–magenta and **19**–cyan). (B) Binding mode of compound **19** in D_3 receptor. (C) Binding mode of compound **18** (*R* enantiomer), and (D) Binding mode of compound **19** (*S* enantiomer), with its the most populated 5-HT_6R conformations obtained by the clustering of the MD trajectories. The $N^{(+)}H\cdots{}^{(-)}O$ cyclic-tertiary amine theoretical interaction sphere illustrates the projected qualities of the formed L−R salt bridge. Interaction energies are represented by bins for which spectrum colors (red to blue to purple) were assigned to denote the interaction energy level.

Analysis of the binding mode of all synthesized derivatives to D_3R indicated that the protonated pyrrolidine moiety created salt bridge with D3.32, the 1*H*-pyrrolo[3,2-*c*]quinoline ring formed CH–π interaction with F6.51, the sulfonamide group was hydrogen bonded with S5.43, and the terminal 3-substituted phenyl ring formed π–π interaction with H6.55 (Figure 3B).

We next focused on the influence of the kind of the alkyl substituent on the basic nitrogen atom of pyrrolidine of CPPQ on the receptors affinity. Introduction of an ethyl moiety, with substituent volume (R volume) equal 44.471 cm^3/mol, slightly decreased affinity for the 5-

HT_6R compared to CPPQ, and maintained affinity the for the D_3R (**12** *vs* CPPQ). Elongation of the alkyl chain to three methylene units (R volume = 54.052 cm^3/mol) decreased affinity for the 5-HT_6R a bit more than **12**, compared to the parent compound (**14** *vs* **12** *vs* CPPQ), however it increased binding at D_3R.

Subsequently, functionalization of CPPQ with a sterically hindered methylenecyclopropyl fragment, which is the substituent of highest tested volume (R volume = 92.791 cm^3/mol), further decreased affinity of the resulting compound for the 5-HT_6R (**17** *vs* CPPQ). On the other hand, the smallersubstituent volume obtained by replacement of methylenecyclopropyl with an *iso*-butyl chain (R volume = 59.21 cm^3/mol) provided a compound with higher affinity for the 5-HT_6R than **17** (**19**, K_i = 27 nM). This compound displayed the highest affinity for D_3R among the evaluated derivatives (**19**, 98.1% at 1 μM). Introduction of a 2-methylbutyl group, with a large substituent volume (R volume = 87.144 cm^3/mol) did not distupt the affinity for the 5-HT_6R (**20**, K_i = 30 nM) compared to **19**, but it slightly decreased affinity for the D_3R.

The influence of the alkyl substituent size on affinity for 5-HT_6R, was further confirmed by *in silico* analysis, which indicated the limitations of the receptor binding pocket. Indeed, closer inspection of the binding modes for all synthesized derivatives showed that the various alkyl chains on the nitrogen atom of pyrrolidine penetrated into the narrow hydrophobic subpocket formed by TM 2, 3, and 7 (Figure 3A). Thus, increased alkyl substituent volume (Table 1) induced potential steric hindrances with larger amino acid side chains (e.g. V2.53, I3.40, C3.36). On the other hand, introduction of alkyl substituent was favorable in terms of interaction with D_3R.

Taking into account the important role of halogen bonding in the interaction with various GPCRs, and specifically the 5-HT_6R,[26–28] the chlorine atom was removed from the arylsulfonyl fragment. This modification confirmed the strong contribution of halogen bonding for binding to the 5-HT_6R (**21** *vs* **14**).

To evaluate the impact of the amidine fragment on the receptor affinity, 3-aminopyrrolidine was replaced with its 3-hydroxy congener. This modification did not significantly affect the interaction in the binding pocket of either 5-HT_6 and D_3Rs (**15** *vs* **14**).

Because the stereochemical properties influence binding of a molecule in the receptor pocket,[34] four pairs of enantiomers were investigated. A strong preference for *S* enantiomers (**12**, **14**, **17**, **19**) over the *R* counterparts (**11**, **13**, **16**, **18**) was observed with respect to their 5-HT_6R affinity. In contrast, *R* enantiomers (**11**, **13**, **16**, **18**) were more favorable for the interaction with the D_3R binding pocket than *S* congeners (**12**, **14**, **17**, **19**).

As revealed by the analysis of the 100 ns-long molecular dynamics trajectories, performed for each pair of enantiomers, the higher 5-HT_6R-binding activity observed for the *S* isomers (**12**, **14**, **17**, **19**) than *R* (**11**, **13**, **16**, **18**) originated from the quality of the salt bridge formed with D3.32. Comparison of the pair of *R* and *S* enantiomers (Figure 3C and 3D respectively) clearly indicated that only with the *S* counterpart did the salt bridge interaction point toward the most positive area of the sphere. The calculated interaction spheres can be used to determine the quality of salt bridge contact in a ligand–protein complex, where the salt bridge plays a crucial role. In all cases, the *S* enantiomers showed distance and angle of the salt bridge that were closer to the mean values reported recently in a multidimensional analysis of salt bridge L–R complexes found in the PDB.[35]

More detailed investigation confirmed high affinity of **19** for D_3R (K_i = 30 nM), and its antagonistic properties (82% inhibition of control agonist at 1 μM, performed at Eurofins) in cAMP cellular assays. Furthermore, compound **19** did not bind to 5-HT_{1A}, 5-HT_{2A}, and or 5-HT_7 receptors and it displayed 10 fold selectivity over D_2Rs (Table 2). Therefore, **19** might be potentially devoid of side effects associated with D_2R blockade, such as extrapyramidal symptoms and prolactin release.

Table 2. Binding data and functional activity of compound **19** for 5-HT_6R and D_3R and binding data for 5-HT_{1A}, 5-HT_{2A}, 5-HT_7 and D_2 receptors.

Compound	K_i [nM][a]		K_i [nM][b]			
	5-HT_6	D_3[c]	5-HT_{1A}	5-HT_{2A}	5-HT_7	D_2
19	27	30	6155	1378	1437	346

[a]Mean K_i values, based on three independent binding experiments (SEM ≤ 37%). [b]Mean K_i values (SEM ≤ 22%) [c]performed at Eurofins.

Functional evaluation of **19** revealed antagonist properties in cAMP assay (K_b = 83 nM) (Figure 4A). In order to determine the influence of compound **19** on 5-HT_6R constitutive activity at Gs signaling,[8,9] derivative **19** was further tested in NG108-165 neuroblastoma cell line, transiently expressing 5-HT_6Rs. Compound **19** did not significantly affect cAMP level, indicating neutral antagonist properties at this signaling path (IC_{50} = 143 μM). On the other hand, intepirdine, the reference 5-HT_6R antagonist strongly decreased basal cAMP level in a concentration-dependent manner and thus behaved as inverse agonist in this model (Figure B).

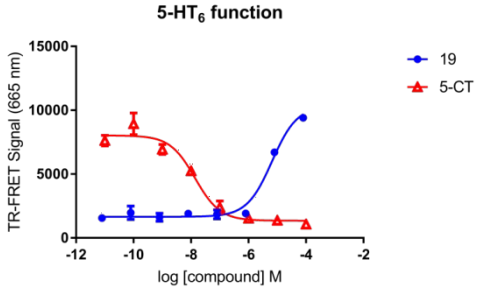

Figure 4A. Functional dose-response curve stimulation/inhibition of production of cAMP. K_b value was calculated from equation: K_b = IC50/(1+A/EC50) where A is the agonist (5-CT) concentration used (1000 nM), IC_{50} is the concentration of antagonist producing a 50% reduction in the response to agonist and EC_{50} (13 nM) is 5-CT concentration which causes a 50% maximal response.

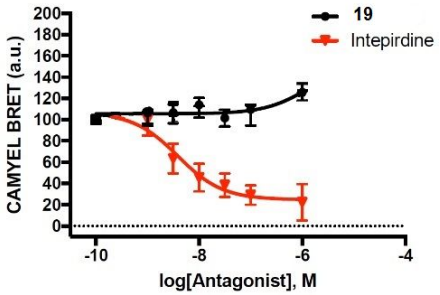

Figure 4B. Influence of compound **19** and intepirdine on the 5-HT_6R constitutive activity at G_s signaling in NG108-15 cells. NG108-15 cells transiently expressing the 5-HT_6R were exposed to incremental concentrations of either intepirdine or **19** for 5 min. Cyclic AMP levels were estimated by BRET using the cAMP sensor CAMYEL. Data are the means ± SEM of the values obtained in three independent experiments that were performed in quadruplicate using different sets of cultured cells. ***p < 0.001 *vs* vehicle (ANOVA followed by Student−Newman−Keuls test).

In addition to its acknowledged role in cognition, the 5-HT_6R is involved in differentiation of neuronal cells through Cdk5-dependent mechanism. It was shown, that expression of the 5-HT_6R in NG108-15 cells induces neurite growth in an agonist-independent manner. Therefore, preventing 5-HT_6R-operated Cdk5 signaling by inverse agonists can inhibit neurite growth. In fact intepirdine, which displayed inverse agonist properties at G_s signaling pathway, strongly reduced NG108-15 cell neurite length. In contrast, neurite length of cells treated with compound **19** did not differ from control cells (Figure 5).

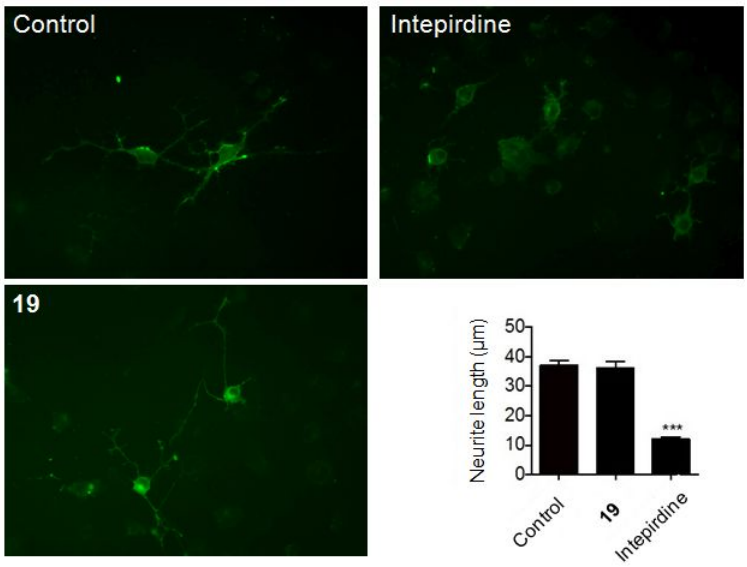

Figure 5. NG108-15 cells were transfected with a plasmid encoding a GFP-tagged 5-HT_6R and exposed to either DMSO (Control), intepirdine (1 µM) or compound **19** (1 µM) for 24 h. The histogram shows the means ±SEM of neurite length in each experimental condition measured from three independent experiments. ***$p < 0.001$ *vs* cells expressing 5-HT_6R and treated with DMSO. Scale bar, 10 µm.

Evaluation of neuroprotective properties

Because the loss of homeostatic function of neuronal cells is an important feature of neurodegenerative diseases[36] derivative **19** was evaluated for its protective properties in C8-D1A astrocytes, a normal cell line derived from mouse cerebellum.

First, the cytotoxicity of **19**, CPPQ and intepirdine was examined using the MTT assay (assess cell metabolic stability) in order to select the safe (nontoxic) concentrations for further analysis (Figure 6A). The results revealed that none of these compounds induced significant cytotoxicity at concentrations up to 1µM, while at larger concentrations, CPPQ and **19** induced a decrease in MTT staining. We next showed that a non-toxic concentration of compound **19**, CPPQ and intepirdine (0.25 µM) protected C8-D1A astrocytes against doxorubicine (DOX) induced cytotoxicity (Figure 6B). These observations were further confirmed measuring LDH release as an index of cell membrane integrity (Figure 6C). Interestingly, the neuroprotective effect of **19** and CPPQ was more marked when the higher concentration of DOX was applied. In contrast, intepirdine did not produce any significant neuroprotective effect (Figure 6C). Given the neuroprotective properties of 1*H*-pyrrolo[3,2-*c*]quinoline derivatives (**19**, CPPQ) in DOX-induced damage of glial cells, this effect warrants more detailed exploration.

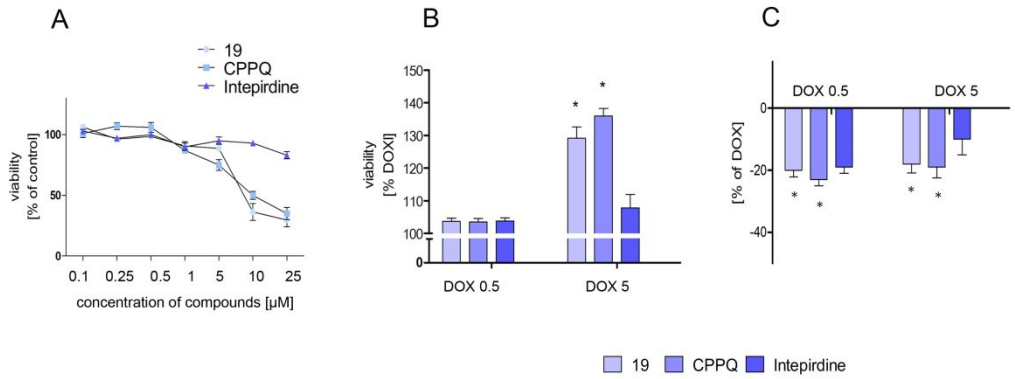

Figure 6. Effect of CPPQ, **19** and intepirdine on DOX-induced astrocyte death (A) Viability of astrocytes treated for 24 h with the indicated compounds applied at 0.1–25 μM concentration range. (B) MTT and (C) LDH assays were performed on astrocytes co-treated with tested compounds in concentration 0.25 μM and DOX for 24 h. Graphs represent the number of viable cells expressed as percent of control (cells incubated with DOX alone). Results are presented as mean ± SD calculated from at least three independent experiments. The statistical significance was determined using non-parametric Mann-Whitney test, with $p < 0.05$ considered to indicate significant differences.

Astrocytes morphology was also examined following exposure to these three compounds (Figure 7). After incubating cells with DOX, cells started to detach from the substrate, shrink and form fewer intracellular connections, effects that were abolished by the co-application of compound **19** and CPPQ (Figure 7).

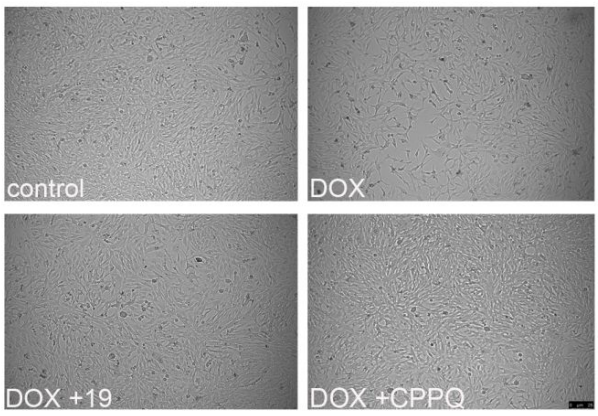

Figure 7. Astrocytes morphology following treatment with either vehicle (control) or DOX in absence or presence of compound **19** (DOX + **19**) or CPPQ (DOX + CPPQ). Pictures were taken using Leica DFC 3000G microscope and are representative of three independent experiments performed with different sets of cultured cells.

***In vivo* pharmacological evaluation**

In order to reveal the potential of obtained compounds for the amelioration of cognitive functions, we next evaluated the ability of compound **19** to reverse PCP-induced memory decline in the NOR task in rats. As expected, rats treated with vehicle but not PCP (5 mg/kg), spent significantly more time exploring the novel object than the familiar one, indicating that PCP abolished the ability to discriminate novel and familiar objects. Following a single administration, **19** significantly inhibited PCP-induced episodic memory decline at doses of 1–3 mg/kg (*ip*) (Figure 8). This effect was comparable with the results obtained for CPPQ, as both compounds fully reversed PCP-induced memory decline at a dose of 3 mg/kg (*i.p.*) in rats,[25] and confirmed the therapeutic potential of dual 5-HT_6/D_3R antagonists in the treatment of cognitive decline.

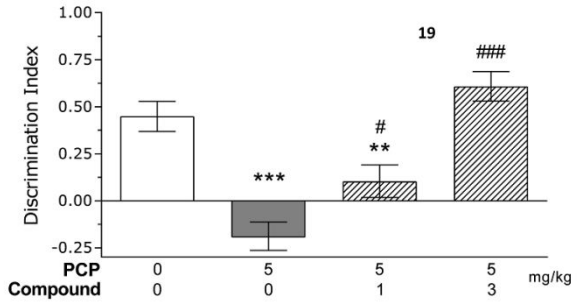

Figure 8. The effects of compound **19** on PCP-induced cognitive impairment in the novel-object recognition test in rats. The data are presented as the mean ± standard error of the mean of discrimination index (DI). N = 6–8 animals per group. Symbols: ** $p < 0.01$, *** $p < 0.001$ significant reduction in DI compared with the vehicle-treated group; # $p < 0.05$, ### $p < 0.001$, significant increase in DI compared with the PCP-treated group.

Conclusions

Applying the concept of dually acting compounds, we designed a novel series of 5-HT_6/D_3R ligands in a group of 1*H*-pyrrolo[3,2-*c*]quinoline. Structure-activity relationship studies, supported by molecular modeling, confirmed that introduction of alkyl chains on the nitrogen atom of pyrrolidine in CPPQ, a previously described 5-HT_6R selective antagonist,[25] maintain high affinity for 5-HT_6R and increase the affinity for D_3 sites. Further analysis of molecular dynamic calculations revealed that stereochemical properties of the molecule strongly affect affinity for 5-HT_6R due to the impact on salt bridge formation. The study identified compound **19** (PZ-1643), a new dual 5-HT_6/D_3R ligand, that behaved as a neutral 5-HT_6R antagonist in cAMP assay and did not affect Cdk5-dependent neurite growth. Moreover,

compound **19** was classified as a D_3R antagonist in cAMP assay and displayed good selectivity over other related monoaminergic receptors tested including 5-$HT_{2A}R$ (being off-target for clinically tested intepirdine). In contrast to intepirdine, both compound **19** and CPPQ showed protective effect against astrocyte damage induced by doxorubicine treatment in tests assessing cell membrane integrity (LDH) and cell metabolic activity (MTT). This observation is of particular significance considering the involvement of glial cells in neurodegenerative processes.[36] This protective effect is an important and interesting feature of evaluated compounds and thus warrants further investigation. Finally, pro-cognitive properties of the dual 5-HT_6/D_3Rs antagonist were demonstrated *in vivo*, since derivative **19** reversed PCP-induced cognitive impairment in NOR test in rats.

Acknowledgements

The authors thank Dr Krzysztof Marciniec for performing HR MS analyses. The study was financed from National Science Center, Poland (grant n° 2016/21/B/NZ7/01742), grant-in-aid for young researchers Jagiellonian University Medical College (n° K/DSC/004286). PM, SCD, FL, XB are supported by grants from CNRS, INSERM, Université de Montpellier, Fondation pour la Recherche Médicale (FRM) and ANR (n° ANR-17-CE16-0010-01 to SCD and n° ANR-17-CE16-0013-01 to PM). Authors acknowledge PHC Polonium programme.

Methods

General methods

The synthesis was carried out at ambient temperature, unless indicated otherwise. Organic solvents (from Aldrich and Chempur) were of reagent grade and were used without purification. The reagents were purchased from Sigma-Aldrich and Fluorochem.

^{1}H NMR and ^{13}C NMR spectra were obtained in a Varian BB 200 spectrometer using TMS (0.00 ppm) and were recorded at 300 MHz and 75 MHz respectively; *J* values are in hertz (Hz), and splitting patterns are designated as follows: s (singlet), d (doublet), t (triplet), m (multiplet).

UPLC/MS were carried out on a system consisting of a Waters Acquity UPLC, coupled to a Waters TQD mass spectrometer. All the analyses were carried out using an Acquity UPLC BEH C18, 100 × 2.1 mm column, at 40°C. A flow rate of 0.3 mL/min and a gradient of (0–100)% B over 10 min was used. Eluent A: water/0.1% HCOOH; eluent B: acetonitrile/0.1% HCOOH. Retention times t_R were given in minutes. The UPLC/MS purity of all the test compounds and key intermediates was determined to be >99%.

High-resolution MS measurements were performed on a Bruker Impact II mass spectrometer (Bruker Corporation, Billerica, USA). Electrospray ionization (ESI) was used in the positive ion mode. Mass accuracy was within 2 ppm error in full-scan mode. The optimized MS parameters were the following: ion spray voltage 4 kV; capillary temperature 240 ºC, dry gas flow rate 4 l/min. High-purity nitrogen as the nebulizing gas was used. Samples of 50 µM concentration were prepared from tested compounds using an eluent of acetonitrile + water (80:20) + 1% HCOOH.

Melting points were determined with Büchi apparatus and are uncorrected.

Elementar analyses for C, H and N were carried out using the elemental Vario El III elemental analyzer (Hanau, Germany). Elemental analyses were found within ±0.4% of the theoretical values.

The synthesis of compounds **2**–**5** was performed according to the previously described procedures.[25]

Compound **19** selected for functional evaluation at 5-HT_6R and D_3R, protection studies and behavioral evaluation was converted into the hydrochloride salt.

General procedure for preparation of compounds 6a and 6b

Compound **5** (0.5 g, 2 mmol, 1 eq) was suspended in 12 ml of MeCN followed by addition of amine (1.3 g, 6.9 mmol, 4 eq). The reaction was performed in microwave at 140°C for 5 h. The solvent was subsequently evaporated and the mixture was purified on silica with DCM/MeOH 9/1.5 (v/v) as a developing solvent.

(*S*)-4-(1-*tert*-Butoxycarbonyl-pyrrolidine-3-yl-amino)-1*H*-pyrrolo-[3,2-*c*]quinoline (6a)

Orange oil, 60%, yield, t_R = 4.38, $C_{20}H_{25}N_4O_2$, MW 352.43. ^{1}H NMR(300 MHz, DMSO-d_6) δ (ppm) 1.35−1.49 (m, 9H), 1.98 (bs, 1H), 2.30 (bs, 1H), 3.27−3.56 (m, 4H), 3.71−3.81 (m, 1H), 4.93 (bs, 1H), 6.55 (d, *J* = 3.08 Hz, 1H), 7.13 (d, *J* = 3.08 Hz, 1H), 7.16−7.23 (m, 1H), 7.25−7.27 (m, 1H), 7.33−7.34 (t, *J* = 7.31 Hz, 1H), 7.71−7.81 (d, *J* = 8.46 Hz, 1H), 7.86 (dd, *J* = 7.95, 1.28 Hz, 1H). Monoiotopic mass 352.19, $[M + H]^+$ 353.2. HRMS calcd for $C_{20}H_{25}N_4O_2$, 353.1978, found, 353.1978.

(*R*)-4-(1-*tert*-Butoxycarbonyl-pyrrolidine-3-yl-amino)-1*H*-pyrrolo-[3,2-*c*]quinoline (6b)

Orange oil, 62% yield, t_R = 4.38, $C_{20}H_{24}N_4O_2$, MW 352.43. ^{1}H NMR (300 MHz, DMSO-d_6) δ (ppm) 1.37−1.50 (m, 9H), 2.00 (bs, 1H), 2.30 (bs, 1H), 3.28−3.56 (m, 4H), 3.70−3.85(m, 1H), 4.92 (bs, 1H), 6.50−5.58 (d, *J* = 3.08 Hz, 1H), 7.10−7.15 (d, *J* = 3.08 Hz, 1H), 7.17−7.24 (m, 1H), 7.25−7.28 (m, 1H), 7.34−7.43(t, *J* = 7.18 Hz, 1H), 7.72−7.82 (d, *J* = 7.95 Hz, 1H), 7.83−7.90 (dd, *J* = 7.95, *J* = 1.03 Hz, 1H). Monoisotopic mass 352.19, $[M + H]^+$ 353.2. HRMS calcd for $C_{20}H_{25}N_4O_2$ 353.1978; found, 353.1978

***tert*-Butyl-(*S*)-3-((1*H*-pyrrolo[3,2-*c*]quinolin-4-yl)oxy)pyrrolidine-1-carboxylate (7)**

To a solution of compound **5** (400 mg, 2 mmol, 1 eq) in DMF (7 ml) and added Cs_2CO_3 (775 mg, 2.38 mmol, 1.2 eq). Benzyl bromide (270 µl, 2.18 mmol, 1.1 eq) was added dropwisely. The reaction was conducted at room temperature for 30 min. Then, the mixture was diluted with AcOEt (15 ml), washed with water (3×) and brine (1×), dried over Na_2SO_4, filtrated and concentrated under reduced pressure. The remaining crude was purified on chromatographic column with AcOEt/Hex 2/8 (v/v) as a developing solvent.

Colorless oil, 80% yield, t_R = 7.72, $C_{18}H_{13}ClN_2$, MW 292.76, Monoisotopic Mass 292.08, $[M+H]^+$ 293.20.1H NMR (300 MHz, $CDCl_3$) δ (ppm) 5.79 (s, 2H), 6.89 (d, *J* = 3.08 Hz, 1H),

7.02–7.08(m, 2H), 7.20 (d, *J* = 3.08 Hz, 1H), 7.24–7.28 (m, 1H), 7.28–7.37 (m, 3H), 7.38–7.42 (m, 1H), 7.52–7.58(m, 1H).

tert-Butyl (*S*)-3-((1-benzyl-1*H*-pyrrolo[3,2-*c*]quinolin-4-yl)oxy)pyrrolidine-1-carboxylate (8)

Derivative **7** (500 mg, 1.71 mmol, 1 eq) was mixed together with $Pd_2(dba)_3$ (31 mg, 0.03 mmol, 0.02 eq), BINAP (42 mg, 0.07 mmol, 0.04 eq) and KO*t*-Bu (268 mg, 2.4 mmol, 1.4 eq). The mixture was suspended in toluene (10 ml) and 1-Boc-3-hydroxypyrrolidine (382 mg, 2.00 mmol, 1.2 eq) was added. The reaction was irradiated by microwaves at 115°C for 1h. The resulting mixture was concentrated and purified on silica gel using AcOEt/Hex 3/7 (v/v) as a developing solvent.

Colorless oil, 80% yield, t_R = 9.16, $C_{27}H_{29}N_3O_3$, MW 443.54, Monoisotopic Mass 443.22, $[M+H]^+$ 444.4. ^{1}H NMR (300 MHz, $CDCl_3$) δ (ppm) 1.47 (s, 9H), 2.22–2.36 (m, 2H), 3.53–3.71 (m, 3H), 3.72–3.90 (m, 2H), 5.76 (s, 2H), 6.79 (d, *J* = 3.08, Hz, 1H), 7.01–7.11 (m, 3H), 7.17–7.24 (m, 1H), 7.27–7.35 (m, 3H), 7.44 (t, *J* = 7.05 Hz, 1H), 7.90 (d, *J* = 7.95 Hz, 2H).

tert-Butyl (*S*)-3-((1*H*-pyrrolo[3,2-*c*]quinolin-4-yl)oxy)pyrrolidine-1-carboxylate (9)

Obtained colorless oil **8** (620 mg, 1.40 mmol, 1 eq) was suspended in DMSO, and KO*t*-Bu (1.25 g, 11.2 mmol, 8 eq) was added as a solid. The flask was placed in the oil bath and the air was bubbled into the mixture. The reaction was carried out at 70°C for 30 min. Next, the mixture was diluted with water and was extracted with AcOEt (3x). After drying over Na_2SO_4 it was concentrated and purified on the silica with AcOEt/Hex 4/6 (v/v) as a developing solvent.

Colorless oil, yield 90%, t_R = 6.47, $C_{20}H_{23}N_3O_3$, MW 353.41, Monoisotopic Mass 353.17, $[M+H]^+$ 354.3. ^{1}H NMR (300 MHz, $CDCl_3$) δ (ppm) 1.47 (s, 9H), 2.25–2.45 (m, 2H), 3.49–3.71 (m, 3H), 3.73–3.90 (m, 2H), 6.70–6.78 (m, 1H), 7.15–7.22 (m, 1H), 7.33–7.43 (m, 1H), 7.51 (t, *J* = 7.44 Hz, 1H), 7.85–7.96 (m, 2H), 9.28 (bs, 1H).

General procedure for preparation of compounds 10a–10e

Compunds **6a**, **6b** and **9** (0.28 mmol, 1 eq), were dissolved in DCM (5 ml) and BTPP (170 µl, 0.56 mmol, 2 eq) was added. The mixture was placed in ice-bath, sulfonyl chloride (1.8 eq) was added, and the reaction mixture was stirred for 3 h. Subsequently, the mixture was evaporated

and the remaining crude product was purified on silica gel. The Boc-protected derivatives were treated with 1 N solution in MeOH to give HCl salts of secondary amines.

(*R*)-1-((3-Chlorophenyl)sulfonyl)-*N*-(pyrrolidin-3-yl)-1*H*-pyrrolo[3,2-*c*]quinolin-4-amine hydrochloride (10a)

White solid, 91% yield, t_R = 4.18, Mp 221-223 °C, $C_{21}H_{19}ClN_4O_2S$, MW 426.92, Monoisotopic Mass 426.09. $[M+H]^+$ 427.2. ^1H NMR (300 MHz, $CDCl_3$) δ (ppm) 2.24–2.40 (m, 1H), 2.52–2.69 (m, 1H), 3.27–3.44 (m, 2H), 3.56–3.79 (m, 3H), 5.46–5.68 (m, 1H), 7.32–7.64 (m, 5H), 7.71 (t, *J* = 1.79 Hz, 1H), 7.85–8.01 (m, 2H), 8.48 (d, *J* = 8.25 Hz, 1H), 8.76 (dd, *J* = 8.53, *J* = 1.10 Hz, 1H). ^{13}C NMR (75 MHz, DMSO-d_6) δ ppm 31.15, 44.21, 49.11, 52.73, 108.81, 112.90, 115.89, 120.21, 123.67, 125.56, 126.40, 127.17, 130.19, 130.66, 132.77, 134.42, 135.29, 136.14, 138.48, 148.45.

(*S*)-1-((3-Chlorophenyl)sulfonyl)-*N*-(pyrrolidin-3-yl)-1*H*-pyrrolo[3,2-*c*]quinolin-4-amine hydrochloride (10b)

White solid, 92% yield, t_R = 4.18, Mp 219-221 °C, $C_{21}H_{19}ClN_4O_2S$, MW 426.92, Monoisotopic Mass 426.09, $[M+H]^+$ 427.2. ^1H NMR (300 MHz, $CDCl_3$) δ (ppm) 2.25–2.38 (m, 1H), 2.54–2.68 (m, 1H), 3.23–3.35 (m, 1H), 3.38–3.43 (m, 1H), 3.57–3.76 (m, 3H), 5.50–5.64 (m, 1H), 7.29–7.63 (m, 5H), 7.71 (t, *J* = 1.80 Hz, 1H), 7.84–7.98 (m, 2H), 8.46 (d, *J* = 8.46 Hz, 1H), 8.75 (dd, *J* = 8.59, *J* = 1.15 Hz, 1H). ^{13}C NMR (75 MHz, DMSO-d_6) δ ppm 31.15, 44.21, 49.11, 52.73, 108.81, 112.90, 115.89, 120.21, 123.67, 125.56, 126.40, 127.17, 130.19, 130.66, 132.77, 134.42, 135.29, 136.14, 138.48, 148.45. HRMS found 427.0984.

(*S*)-1-(Phenylsulfonyl)-*N*-(pyrrolidin-3-yl)-1*H*-pyrrolo[3,2-*c*]quinolin-4-amine hydrochloride (10c)

White solid, 80% yield, t_R = 4.78, Mp 220–222 °C, $C_{21}H_{20}N_4O_2S$, MW 392.47, Monoisotopic Mass: 392.13, $[M+H]^+$ 393.1. ^1H NMR (300 MHz, DMSO-d_6) δ (ppm) 2.21 (d, *J* = 4.98 Hz, 1H), 2.31–2.45 (m, 1H), 3.56 (d, *J* = 4.98 Hz, 5H), 5.28 (bs, 1H), 7.44 (d, *J* = 7.04 Hz, 1H), 7.55–7.65 (m, 3H), 7.68–7.77 (m, 1H), 7.92 (d, *J* = 7.62 Hz, 2H), 8.19 (d, *J* = 3.52 Hz, 1H), 8.65 (d, *J* = 7.92 Hz, 1H), 9.50 (bs, 2H).

(*S*)-1-((3-Fluorophenyl)sulfonyl)-*N*-(pyrrolidin-3-yl)-1*H*-pyrrolo[3,2-*c*]quinolin-4-amine hydrochloride (10d)

White solid, 85% yield, t_R = 3.95, Mp 197–199 °C, $C_{21}H_{19}FN_4O_2S$, MW 410.46, Monoisotopic Mass: 410.12, $[M+H]^+$ 411.3. ^{1}H NMR (300 MHz, DMSO-d_6) δ (ppm) 2.21 (d, *J* = 4.69 Hz, 1H), 2.40 (dd, *J* = 13.93, 6.89 Hz, 1H), 3.26–3.35 (m, 2H), 3.52–3.59 (m, 3H), 5.28 (bs, 1H), 7.47 (d, *J* = 7.33 Hz, 1H), 7.58–7.69 (m, 3H), 7.77 (d, *J* = 7.04 Hz, 1H), 7.94 (d, *J* = 7.92 Hz, 1H), 8.05 (bs, 1H), 8.18 (d, *J* = 3.52 Hz, 1H), 8.39 (bs, 1H), 8.63 (d, *J* = 8.21 Hz, 1 H), 9.51 (bs, 2H).

(*S*)-1-((3-Chlorophenyl)sulfonyl)-4-(pyrrolidin-3-yloxy)-1*H*-pyrrolo[3,2-*c*]quinoline hydrochloride (10e)

White solid, 87% yield, t_R = 4.23, Mp 225-227 °C, $C_{21}H_{19}ClN_3O_3S$, MW 464.36, Monoisotopic Mass 463.05, $[M+H]^+$ 464.0. ^{1}H NMR (300 MHz, $CDCl_3$) δ (ppm) 2.27–2.39 (m, 1H), 2.58–2.70 (m, 1H), 3.20–3.38 (m, 1H), 3.41–3.45 (m, 1H), 3.59–3.79 (m, 3H), 5.52–5.68 (m, 1H), 7.33–7.63 (m, 5H), 7.74 (m, 1H), 7.88–8.02 (m, 2H), 8.48 (d, *J* = 8.46 Hz, 1H), 8.78 (dd, *J* = 8.59, *J* = 1.15 Hz, 1H).

General procedure for preparation of final compounds 11–21.

Compounds **10a**–**10e** (80 mg, 1eq) were dissolved in EtOH and respective aldehyde (1.8 eq) were added. The mixture was stirred for 30 min at room temperature and $NaBH_3CN$ (2 eq) was added portiowise. The reaction was performed for 3 hours. Subsequently the mixture was evaporated and the remaining crude product was purified by flash chromatography using water/MeCN as a developing solvent. Collected fractions were evaporated and lyophilized. Compound **19** was treated with 1N HCl in methanol to give final product as HCl salt.

(*R*)-1-((3-Chlorophenyl)sulfonyl)-*N*-(1-ethylpyrrolidin-3-yl)-1*H*-pyrrolo[3,2-*c*]quinolin-4-amine (11)

Colorless oil, 70% yield, t_R = 1.34, $C_{23}H_{23}ClN_4O_2S$, MW 454.97. ^{1}H NMR (300 MHz, CD_3OD) δ (ppm) 1.39 (t, *J* = 7.06 Hz, 3H), 2.36−2.50 (m, 1H), 2.61−2.89 (m, 1H), 3.36 (q, *J* = 6.84 Hz, 2H), 3.43−3.74 (m, 2H), 3.75−4.07 (m, 2H), 5.14 (br.s., 1H), 7.43−7.55 (m, 3H), 7.60−7.67 (m, 2H), 7.73−7.82 (m, 1H), 7.89 (t, *J* = 2.05 Hz, 1H), 7.98 (d, *J* = 8.81 Hz, 1H), 8.11 (d, *J* = 3.52 Hz, 1H), 8.80 (dd, *J* = 8.19, 1.16 Hz, 1H). Monoisotopic Mass 454.12. $[M+H]^+$ HRMS calcd for $C_{23}H_{23}ClN_4O_2S$, 454.1230; found, 455.1304.

(*S*)-1-((3-Chlorophenyl)sulfonyl)-*N*-(1-ethylpyrrolidin-3-yl)-1*H*-pyrrolo[3,2-*c*]quinolin-4-amine (12)

Colorless oil, 68% yield, t_R = 1.34, $C_{23}H_{23}ClN_4O_2S$, MW 454.97. ^{1}H NMR (300 MHz, CD3OD) δ (ppm) 1.39 (t, *J* = 7.00 Hz, 3H), 2.35−2.50 (m, 1H), 2.59−2.91 (m, 1H), 3.36 (q, *J* = 6.84 Hz, 2H), 3.43−3.75 (m, 2H), 3.76−4.07 (m, 2H), 5.14 (br. s., 1H), 7.43−7.56 (m, 3H), 7.59−7.68 (m, 2H), 7.73−7.82 (m, 1H), 7.89 (t, *J* = 2.05 Hz, 1H), 7.98 (d, *J* = 8.79 Hz, 1H), 8.11 (d, *J* = 3.5 Hz, 1H), 8.80 (dd, *J* = 8.21, 1.17 Hz, 1H) Monoisotopic Mass 454.12. $[M+H]^+$ 455.4. HRMS calcd for $C_{23}H_{23}ClN_4O_2S$, 454.1230; found, 455.1311.

(*R*)-1-((3-Chlorophenyl)sulfonyl)-*N*-(1-propylpyrrolidin-3-yl)-1*H*-pyrrolo[3,2-*c*]quinolin-4 amine (13)

Colorless oil, 65% yield, t_R = 1.36, $C_{24}H_{25}ClN_4O_2S$, MW 469.0. ^{1}H NMR (300 MHz, CD_3OD) δ (ppm) 1.02 (t, *J* = 7.33 Hz, 3H), 1.36−1.45 (m, 1H), 1.70−1.88 (m, 2H), 2.26−2.48 (m, 1H), 2.54−2.77 (m, 1H), 3.14−3.27 (m, 2H), 3.35−3.68 (m, 2H), 3.72−4.08 (m, 2H), 7.19−7.37 (m, 2H), 7.42−7.57 (m, 2H), 7.62 (dd, *J* = 8.21, 1.17 Hz, 1H), 7.67−7.79 (m, 2H), 7.81 (t, *J* = 2.05 Hz, 1H), 8.02 (d, *J* = 3.52 Hz, 1H), 8.80 (d, *J* = 8.21 Hz, 1H). Monoisotopic Mass 468.14. $[M+H]^+$ 469.2. HRMS calcd for $C_{24}H_{25}ClN_4O_2S$, 468.1387; found, 469.1462.

(*S*)-1-((3-Chlorophenyl)sulfonyl)-*N*-(1-propylpyrrolidin-3-yl)-1*H*-pyrrolo[3,2-*c*]quinolin-4-amine (14)

Colorless oil, 57% yield, t_R = 1.36, $C_{24}H_{25}ClN_4O_2S$, MW 469.0. ^{1}H NMR (300 MHz, CD_3OD) δ (ppm) 1.03 (t, *J* = 7.33 Hz, 3H), 1.37−1.47 (m, 1H), 1.76−1.85 (m, 2H), 2.31−2.46 (m, 1H), 2.61−2.79 (m, 1H), 3.12−3.26 (m, 2H), 3.43−3.67 (m, 2H), 3.77−4.07 (m, 2H), 7.37−7.46 (m, 2H), 7.51 (t, *J* = 8.21 Hz, 1H), 7.55−7.73 (m, 3H), 7.79 (d, *J* = 8.21 Hz, 1H), 7.88 (t, *J* = 1.76 Hz, 1H), 8.11 (d, *J* = 3.52 Hz, 1H), 8.85 (dd, *J* = 8.79, 1.17 Hz, 1H). Monoisotopic Mass 468.14. $[M+H]^+$ 469.1. HRMS calcd for $C_{24}H_{25}ClN_4O_2S$, 468.1387; found, 469.1465.

(*S*)-1-((3-Chlorophenyl)sulfonyl)-4-((1-propylpyrrolidin-3-yl)oxy)-1*H*-pyrrolo[3,2-*c*]quinoline (15)

Colorless oil, 73.3% yield, t_R=1.72, $C_{24}H_{24}ClN_3O_3S$, MW 469.98. ^{1}H NMR (300 MHz, CD_3OD) δ (ppm) 1.02 (t, *J* = 7.33 Hz, 3H), 1.67−1.86 (m, 2H), 2.38−2.59 (m, 1H), 2.64−2.87 (m, 1H), 3.24 (dd, *J* = 3.81, 2.05 Hz, 2H), 3.40−3.70 (m, 2H), 3.75−4.11 (m, 2H), 5.89−6.05 (m, 1H), 7.07 (d, *J* = 3.52 Hz, 1H), 7.41−7.50 (m, 2H), 7.53−7.64 (m, 2H), 7.70−7.76 (m, 1H), 7.81 (t, *J* = 1.76 Hz, 1H), 7.87 (dd, *J* = 8.21, 1.17 Hz, 1H), 8.03 (d, *J* = 3.52 Hz, 1H), 8.91 (dd,

J = 8.21, 1.17 Hz, 1H). Monoisotopic Mass 469.12. $[M+H]^+$ 470.98. HRMS calcd for $C_{24}H_{24}ClN_3O_3S$, 469.1227; found, 470.1303.

(*R*)-1-((3-Chlorophenyl)sulfonyl)-*N*-(1-(cyclopropylmethyl)pyrrolidin-3-yl)-1*H*-pyrrolo[3,2-*c*]quinolin-4-amine (16)

Colorless oil, 47% yield, t_R = 1.38, $C_{25}H_{25}ClN_4O_2S$, MW 481.01. ^{1}H NMR (300 MHz, CD_3OD) δ (ppm) 0.42−0.52 (m, 2H), 0.68−0.82 (m, 2H), 1.08−1.24 (m, 1H), 1.26−1.49 (m, 1H), 2.32−2.50 (m, 1H), 2.55−2.88 (m, 1H), 3.21 (d, J = 7.03 Hz, 2H), 3.45−3.76 (m, 2H), 3.88−4.10 (m, 2H), 5.01−5.12 (m, 1H), 7.43−7.57 (m, 3H), 7.60−7.72 (m, 2H), 7.82 (d, J = 8.21 Hz, 1H), 7.92 (t, J = 1.76 Hz, 2H), 8.16 (d, J = 4.10 Hz, 1H), 8.87 (dd, J = 8.79, 1.17 Hz, 1H). Monoisotopic Mass 480.14. $[M+H]^+$ 481.1. HRMS calcd for $C_{24}H_{25}ClN_4O_2S$, 480.1387; found, 481.1462.

(*S*)-1-((3-Chlorophenyl)sulfonyl)-*N*-(1-(cyclopropylmethyl)pyrrolidin-3-yl)-1*H*-pyrrolo[3,2-*c*]quinolin-4-amine (17)

Colorless oil, 64% yield, t_R = 1.38, $C_{25}H_{25}ClN_4O_2S$, MW 481.01. ^{1}H NMR (300 MHz, CD_3OD) δ (ppm) 0.42−0.52 (m, 2H), 0.68−0.80 (m, 2H), 1.11−1.24 (m, 1H), 1.38−1.47 (m, 1H), 2.32−2.50 (m, 1H), 2.63−2.87 (m, 1H), 3.21 (d, J = 7.03 Hz, 2H), 3.44−3.72 (m, 2H), 3.78−4.11 (m, 2H), 4.98−5.12 (m, 1H), 7.42−7.55 (m, 3H), 7.61−7.71 (m, 2H), 7.82 (d, J = 7.62 Hz, 1H), 7.91 (t, J = 1.76 Hz, 2H), 8.15 (d, J = 3.52 Hz, 1H), 8.87 (dd, J = 8.79, 1.17 Hz, 1H). Monoisotopic Mass 480.14. $[M+H]^+$ 481.0. HRMS calcd for $C_{24}H_{25}ClN_4O_2S$, 480.1387; found, 481.1462.

(*R*)-1-((3-Chlorophenyl)sulfonyl)-*N*-(1-isobutylpyrrolidin-3-yl)-1*H*-pyrrolo[3,2-*c*]quinolin-4-amine (18)

Colorless oil, 56% yield, t_R = 1.41, $C_{25}H_{27}ClN_4O_2S$ MW 483.03. ^{1}H NMR (300 MHz, CD_3OD) δ (ppm) 1.00−1.11 (m, 6H), 1.36−1.49 (m, 1H), 2.04−2.19 (m, 1H), 2.33−2.48 (m, 1H), 2.55−2.85 (m, 1H), 3.13−3.24 (m, 2H), 3.40−3.69 (m, 2H), 3.74−4.09 (m, 2H), 7.36−7.56 (m, 3H), 7.57−7.70 (m, 2H), 7.80 (d, J = 7.62 Hz, 1H), 7.89 (t, J = 2.30 Hz, 2H), 8.13 (d, J = 2.92 Hz, 1H), 8.86 (d, J = 8.21 Hz, 1H). Monoisotopic Mass 482.15. $[M+H]^+$ 483.2. HRMS calcd for $C_{25}H_{27}ClN_4O_2S$, 482.1543; found, 483.1620.

(*S*)-1-((3-Chlorophenyl)sulfonyl)-*N*-(1-isobutylpyrrolidin-3-yl)-1*H*-pyrrolo[3,2-

***c*]quinolin-4-amine (19)**

Colorless oil, 50% yield, t_R = 1.41, $C_{25}H_{28}Cl_2N_4O_2S$, MW 519.49. ^{1}H NMR (300 MHz, CD_3OD) δ (ppm) 1.06 (dd, *J* = 6.45, 3.52 Hz, 6H), 1.21−1.44 (m, 1H), 2.04−2.18 (m, 1H), 2.34−2.50 (m, 1H), 2.56−2.85 (m, 1H), 3.09−3.26 (m, 2H), 3.39−3.77 (m, 2H), 3.79−4.14 (m, 2H), 5.03−5.16 (m, 1H), 7.44−7.58 (m, 3H), 7.61−7.72 (m, 2H), 7.83 (d, *J* = 8.21 Hz, 1H), 7.93 (t, *J* = 1.76 Hz, 2H), 8.17 (d, *J* = 3.52 Hz, 1H), 8.87 (d, *J* = 7.62 Hz, 1H). Monoisotopic Mass 482.15. $[M+H]^+$ 483.5. HRMS calcd for $C_{25}H_{27}ClN_4O_2S$, 482.1543; found, 483.1620.

Compound **19** was converted into HCl salt upon HCl treatment in MeOH. Mp for $C_{25}H_{28}Cl_2N_4O_2S{\cdot}HCl$: 187.2−189.4. ^{1}H NMR (300 MHz, CD_3OD) δ (ppm) 1.05 (m, 6H), 1.23−1.40 (m, 1H), 2.00−2.10 (m, 1H), 2.30−2.44 (m, 1H), 2.51−2.83 (m, 1H), 3.02−3.22 (m, 2H), 3.42−3.77 (m, 2H), 3.82−4.18 (m, 2H), 5.01−5.20 (m, 1H), 7.46−7.61 (m, 3H), 7.61−7.72 (m, 2H), 7.83 (m, 1H), 7.93 (t, *J* = 1.76 Hz, 2H), 8.17 (m, 1H), 8.87 (d, *J* = 7.58 Hz, 1H). Anal. calcd. for $C_{25}H_{28}Cl_2N_4O_2S{\cdot}HCl$: C: 57.80, H: 5.43, N: 10.79, S: 6.17; Found: C: 57.92, H: 5.38, N: 10.91, S: 6.04. Mp for $C_{25}H_{28}Cl_2N_4O_2S{\cdot}HCl$: 187.2−189.4.

(*S*)-1-((3-Chlorophenyl)sulfonyl)-*N*-(1-(2-methylbutyl)pyrrolidin-3-yl)-1*H*-pyrrolo[3,2-*c*]quinolin-4-amine (20)

Colorless oil, 66% yield, t_R = 1.45, $C_{26}H_{29}ClN_4O_2S$, MW 497.05. ^{1}H NMR (300 MHz, CD_3OD) δ (ppm) 0.89−1.01 (m, 3H), 1.03−1.10 (m, 3H), 1.16−1.37 (m, 2H), 1.45−1.60 (m, 1H), 1.80−2.00 (m, 1H), 2.32−2.50 (m, 1H), 2.54−2.88 (m, 1H), 3.10−3.27 (m, 2H), 3.39−3.75 (m, 2H), 3.78−4.10 (m, 2H), 5.01−5.16 (m, 1H), 7.43−7.57 (m, 3H), 7.60−7.73 (m, 2H), 7.83 (d, *J* = 7.62 Hz, 1H), 7.89−8.04 (m, 2H), 8.17 (d, *J* = 3.52 Hz, 1H), 8.88 (d, *J* = 8.21 Hz, 1H). Monoisotopic Mass 496.17. $[M+H]^+$ 497.4. HRMS calcd for $C_{26}H_{29}ClN_4O_2S$, 496.1700; found, 497.1776.

(*S*)-1-(Phenylsulfonyl)-*N*-(1-propylpyrrolidin-3-yl)-1*H*-pyrrolo[3,2-*c*]quinolin-4-amine (21)

Colorless oil, 56% yield, t_R = 1.27, $C_{24}H_{26}N_4O_2S$, MW 434.56. ^{1}H NMR (300 MHz, CD_3OD) δ (ppm) 1.04 (t, *J* = 7.33 Hz, 3H), 1.37−1.48 (m, 1H), 1.71−1.88 (m, 2H), 2.30−2.50 (m, 1H), 2.62−2.92 (m, 1H), 3.17−3.28 (m, 2H), 3.41−3.74 (m, 2H), 3.78−4.07 (m, 2H), 5.05−5.19 (m, 1H), 7.46−7.60 (m, 4H), 7.62−7.72 (m, 2H), 7.85−8.02 (m, 3H), 8.19 (d, *J* = 3.52 Hz, 1H), 8.90

(dd, $J = 9.38$, 8.2 Hz, 1H). Monoisotopic Mass 434.18. $[M+H]^+$ 435.5. HRMS calcd for $C_{24}H_{26}N_4O_2S$, 434.1776; found, 435.1848.

In silico evaluation

Structures of the Receptors

The 5-HT_6R homology models built on β2 adrenergic template and successfully used in our previous study to support the structure-activity relationship analysis were used.[27,37,38] The structure of D_3R in complex with antagonist eticlopride (PDB code: 3PBL) was retrieved from the Protein Data Bank.[39]

Molecular Docking

The 3-dimensional structures of the ligands were prepared using LigPrep v3.6,[40] and the appropriate ionization states at pH=7.4±1.0 were assigned using Epik v3.4.[41] The Protein Preparation Wizard was used to assign the bond orders, appropriate amino acid ionization states and to check for steric clashes. The receptor grid was generated (OPLS3 force field)[42] by centering the grid box with a size of 12 Å on D3.32 side chain. Automated flexible docking was performed using Glide v6.9[43] at the SP level, and ten poses per ligand was generated.

Optimization of the Binding Site Using Induced-Fit Docking Procedure

The structure of the 5-HT_6 and D3 receptors were optimized using the induced-fit docking (IFD)[44,45] procedure from Schrödinger Suite. The IFD combines flexible ligand docking, using the Glide algorithm with receptor structure prediction and side chain refinement in Prime. The structures of four pairs of enantiomers (**11**–**14**, **16**–**19**) were used as inputs to IFD. In each case, the centroid of the grid box was anchored on D3.32 and allowed on residues refinement within 12 Å of ligand poses. Ten top-scored L–R complexes per enantiomer were visually inspected to select those showing the closest compliance with the common binding mode for monoaminergic receptor ligands.[46]

QM/MM Optimization

The L–R complexes selected in IFD procedure were next optimized using QM/MM approach using QSite.[47,48] The QM area containing ligand and the D3.32 amino acid side chain was

described by a combination of DFT hybrid functional B3LYP and LACVP* basis set, while the rest of the system was optimized using OPLS2005 force field.

Molecular Dynamics

A 100 ns-long molecular dynamics (MD) simulations were performed using Schrödinger Desmond software.[49] Each ligand–receptor complex, optimized in QM/MM procedure, was immersed into a POPC (300 K) membrane bilayer, which position was calculated using the PPM web server (accessed Aug 15, 2018).[50] The system was solvated by water molecules described by the TIP4P potential and the OPLS3 force field was used for all atoms. 0.15 M NaCl was added to mimic the ionic strength inside the cell.

The output trajectories were hierarchically clustered into 10 groups according to the ligand using the trajectory analysis tool from Schrödinger Suite. Based on obtained trajectories, the mean geometrical parameters of the salt bridge (distance and angle) with D3.32 were calculated using Simulation Event Analysis tool in Maestro Schrödinger Suite.

Plotting Interaction Spheres for Salt Bridge

To visualize the possible contribution of salt bridge interaction to L−R complex, the previously calculated interaction sphere[35] for cyclic-tertiary amine model was plotted onto the carbonyl oxygen atom of D3.32 in 5-HT_6 and D_3 receptors.[35] For visualization purposes our in-house python script was used.

In vitro pharmacology

Cell culture and preparation of cell membranes for radioligand binding assays

All the experiments were carried our according to the previously published procedures.[32,51,52] HEK293 cells with stable expression of human 5-HT_{1A}, 5-HT_{2A}, 5-HT_6, 5-HT_{7b} and D_{2L} receptors (prepared with the use of Lipofectamine 2000) or CHO-K1 cells with plasmid containing the sequence coding for the human serotonin 5-HT_{2A} receptor (Perkin Elmer) were maintained at 37°C in a humidified atmosphere with 5% CO_2 and grown in Dulbecco's Modifier Eagle Medium containing 10% dialyzed fetal bovine serum and 500 μ/ml G418 sulfate. For membrane preparation, cells were subcultured in 150 cm^2 flasks, grown to 90% confluence, washed twice with phosphate buffered saline (PBS) prewarmed to 37°C and pelleted by centrifugation (200 g) in PBS containing 0.1 mM EDTA and 1 mM dithiothreitol. Prior to membrane preparation, pellets were stored at –80°C.

Radioligand binding assays

The cell pellets were thawed and homogenized in 10 volumes of assay buffer using an Ultra Turrax tissue homogenizer, and were centrifuged twice at 35,000 g for 15 min at 4°C and were incubated for 15 min at 37 °C between centrifugation rounds. The composition of the assay buffers was as follows: for 5-HT_{1A}R: 50 mM Tris HCl, 0.1 mM EDTA, 4 mM $MgCl_2$, 10 μM pargyline and 0.1% ascorbate; for 5-HT_{2A}R: 50 mM Tris HCl, 0.1 mM EDTA, 4 mM $MgCl_2$ and 0.1% ascorbate; for 5-HT_6R: 50 mM Tris HCl, 0.5 mM EDTA and 4 mM $MgCl_2$, for 5-HT_{7b}R: 50 mM Tris HCl, 4 mM $MgCl_2$, 10 μM pargyline and 0.1% ascorbate; for dopamine D_{2L}R: 50 mM Tris HCl, 1 mM EDTA, 4 mM $MgCl_2$, 120 mM NaCl, 5 mM KCl, 1.5 mM $CaCl_2$ and 0.1% ascorbate. All assays were incubated in a total volume of 200 μL in 96-well microtitre plates for 1 h at 37°C, except for 5-HT_{1A}R and 5-HT_{2A}R, which were incubated at room temperature and 27°C, respectively. The process of equilibration was terminated by rapid filtration through Unifilter plates with a 96-well cell harvester, and radioactivity retained on the filters was quantified on a Microbeta plate reader (PerkinElmer, USA). For displacement studies, the assay samples contained as radioligands (PerkinElmer, USA): 2.5 nM [^{3}H]-8-OH-DPAT (135.2 Ci/ mmol) for 5-HT_{1A}R; 1 nM [^{3}H]-ketanserin (53.4 Ci/mmol) for 5-HT_{2A}R; 2 nM [^{3}H]-LSD (83.6 Ci/mmol) for 5-HT_6R; 0.8 nM [^{3}H]-5-CT (39.2 Ci/mmol) for 5-HT_7R or 2.5 nM [^{3}H]-raclopride (76.0 Ci/mmol) for D_{2L}R. Non-specific binding was defined with 10 μM of 5-HT in 5-HT_{1A}R and 5-HT_7R binding experiments, whereas 20 μM of mianserin, 10 μM of methiothepine or 10 μM of haloperidol were used in 5-HT_{2A}R, 5-HT_6R and D_{2L}R assays, respectively. Each compound was tested in triplicate at 7 concentrations (10^{-10}-10^{-4} M). The inhibition constants (K_i) were calculated from the Cheng-Prusoff equation.[53] Results were expressed as means of at least two separate experiments.

Evaluation of functional activity on 5-HT_6Rs

The functional properties of compound **19** on 5-HT_6R was evaluated using its ability to inhibit cAMP production induced by 5-CT (1000 nM) – a 5-HT_6R agonist. Compound was tested in triplicate at 8 concentrations (10^{-11} – 10^{-4} M). The level of adenylyl cyclase activity was measured using frozen recombinant 1321N1 cells expressing the Human Serotonin 5-HT_6R (PerkinElmer). Total cAMP was measured using the LANCE cAMP detection kit (PerkinElmer), according to the manufacture's directions. For quantification of cAMP levels, cells (5 μl) were incubated with mixture of compounds (5 μl) for 30 min at room temperature in 384-well white opaque microtiter plate. After incubation, the reaction was stopped and cells were lysed by the addition of 10 μl working solution (5 μl Eu-cAMP and 5 μl ULight-anti-

cAMP). The assay plate was incubated for 1h at room temperature. Time-resolved fluorescence resonance energy transfer (TR-FRET) was detected by an Infinite M1000 Pro (Tecan) using instrument settings from LANCE cAMP detection kit manual.

Determination of cAMP production as 5-HT_6R constitutive activity

cAMP measurement was performed in NG108-15 cells transiently expressing 5-HT_6R using the Bioluminescence Resonance Energy Transfer (BRET) sensor for cAMP, CAMYEL (cAMP sensor using YFP-Epac-RLuc).[53] NG108-15 cells were co-transfected in suspension with 5-HT_6Rand CAMYEL constructs, using Lipofectamine 2000, according to the manufacturer protocol, and plated in white 96-well plates (Greiner), at a density of 80,000 cells per well. 24 hours after transfection, cells were washed with PBS containing calcium and magnesium. Coelanterazine H (Molecular Probes) was added at a final concentration of 5 μM, and left at room temperature for 5 minutes. BRET was measured using a Mithras LB 940 plate reader (Berthold Technologies). Compound **19** was tested as HCl salt.

Impact of compounds upon neurite growth

NG108-15 cells were grown in Dulbecco's modified Eagle's medium (DMEM) supplemented with 10% dialyzed foetal calf serum, 2% hypoxanthine/aminopterin/thymidine (Life technologies), and antibiotics. Cells were transfected with plasmids encoding either cytosolic GFP or a GFP-tagged 5-HT_6R in suspension using Lipofectamine 2000 (Life technologies) and plated on glass coverslips. Six hours after transfection, cells were treated with either DMSO (control), or compound 17 or intepirdine (1 μM) for 24 h. Cells were fixed in 4% paraformaldehyde (PFA) supplemented with 4% sucrose for 10 min. PFA fluorescence was quenched by incubating the cells in PBS containing 0,1M Glycine, prior to mounting in Prolong Gold antifade reagent (Thermo Fisher Scientific). Cells were imaged using an AxioImagerZ1 microscope equipped with epifluorescence (Zeiss), using a 20 X objective for cultured cells and neurite length was assessed using the Neuron J plugin of the ImageJ software (NIH).

***In vitro* evaluation of protective properties of compounds**

In vitro studies protection studies were designed according to literature and modified for individual purpose.[54–57]

Cell culture

The C8-D1A astrocytes (CRL 25-47) cell line obtained from ATCC was cultured in 25 cm2 flask with DMEM supplemented with 10% FBS at 37°C, in a humidified atmosphere with 5% CO_2 until the cells reached a confluence between 80–90 %. The astrocytes were seeded in 96-well plates with density of $1 \cdot 10^4$ cells per well. For protection studies, astrocytes were co-treated with the cytotoxic agent (DOX) and analyzed compounds (CPPQ, **19**, Intepirdine) for 24 h, then the ability of compounds to protect astrocytes against DOX-induced toxicity was examined using cytotoxicity assays (MTT/LDH).

Cytotoxicity assays

MTT

The cytotoxicity effect was investigated using MTT test, which determined mitochondrial metabolism in living cells in vitro. Cell viability was measured based on alteration of MTT to purple formazan contents by mitochondrial dehydrogenases (enzymes that are active in living cells). MTT reagent was added to each wells. After 4 h of incubation, formazan crystals were then solubilized with 10% SDS and kept for 6 hours at 37°C. OD was measured at 570 nm by using a SpectraMax iD3 Multi-Mode microplate Reader (Molecular Devices). The absorbance was proportional to the number of metabolically active (viable) cells. Each experiment was performed in triplicate and repeated three times. The results were expressed as percentage of control.

LDH

For Lactate Dehydrogenase (LDH) cytotoxicity test (Clonetech), C8-D1A astrocytes were seeded into 96-well plate (Corning) at 1×10^4 cells/cm^2, grown for 24 h and co-treated with the agents and DOX for the next 24 h. The plates were then centrifuged at 250×g for 10 minutes and 100 µl of the supernatant was removed carefully from each well and transferred into the corresponding wells of an optically clear 96-well flat-bottom plate. Next, 100 µl of freshly prepared Reaction Mixture was added to each well and incubated in darkness for up to 30 minutes at room temperature. Absorbance of the samples was measured at 492 nm using the SpectraMax iD3 Multi-Mode Microplate Reader. Cytotoxicity was measured as (%) = (triplicate absorbance-low control/high control-low control)×100. Three independent experiments were performed for each condition.

***In vivo* pharmacology**

Novel object recognition protocol

Procedures based on earlier studies of Popik *et al.*[58] The experiments were conducted in accordance with the NIH Guide for the Care and Use of Laboratory Animals and were approved by the Ethics Committee for Animal Experiments, Institute of Pharmacology.

Male Sprague–Dawley rats (Charles River, Germany) weighing ~250 g at the arrival were housed in the standard laboratory cages, under standard colony A/C controlled conditions: room temperature 21 ± 2°C, humidity (40–50 %), 12-hr light/dark cycle (lights on: 06:00) with ad libitum access to food and water. Rats were allowed to acclimatize for at least 7 days before the start of the experimental procedure. During this week animals were handled for at least 3 times. Behavioral testing was carried out during the light phase of the light/dark cycle. At least 1 h before the start of the experiment, rats were transferred to the experimental room for acclimation. Rats were tested in a dimly lit (25 lx) "open field" apparatus made of a dull gray plastic (66 × 56 × 30 cm). After each measurement, the floor was cleaned and dried.

Procedure consisted of habituation to the arena (without any objects) for 5 min, 24 hours before the test and test session comprised of two trials separated by an inter trial interval (ITI). For phencyclidine (PCP)-induced memory impairment paradigm, 1 hour ITI was chosen. During the first trial (familiarization, T1) two identical objects (A1 and A2) were presented in opposite corners, approximately 10 cm from the walls of the open field. In the second trial (recognition, T2) one of the objects was replaced by a novel one (A=familiar and B=novel). Both trials lasted 3 min and animals were returned to their home cage after T1. The objects used were the glass beakers filled with the gravel and the plastic bottles filled with the sand. The heights of the objects were comparable (~12 cm) and the objects were heavy enough not to be displaced by the animals. The sequence of presentations and the location of the objects was randomly assigned to each rat. The animals explored the objects by looking, licking, sniffing or touching the object while sniffing, but not when leaning against, standing or sitting on the object. Any rat spending less than 5 s exploring the two objects within 3 min of T1 or T2 was eliminated from the study. Exploration time of the objects and the distance traveled were measured using the Any-maze® video tracking system. Based on exploration time (E) of two objects during T2, discrimination index (DI) was calculated according to the formula: DI = (EB–EA)/(EA+AB). Phencyclidine, used to attenuate learning, was administered at the dose of 5 mg/kg (*ip*) 45 before familiarization phase (T1). The compound **19** was administrated *ip* 75 min before familiarization phase (T1).

References

(1) Millan, M. J.; Agid, Y.; Brüne, M.; Bullmore, E. T.; Carter, C. S.; Clayton, N. S.; Connor, R.; Davis, S.; Deakin, B.; Derubeis, R. J.; *et al.* Cognitive Dysfunction in Psychiatric Disorders: Characteristics, Causes and the Quest for Improved Therapy. *Nat. Rev. Drug Discov.* **2012**, *11* (2), 141–168.

(2) Medina-Franco, J. L.; Giulianotti, M. A.; Welmaker, G. S.; Houghten, R. A. Shifting from the Single to the Multitarget Paradigm in Drug Discovery. *Drug Discov. Today* **2013**, *18* (9), 495–501.

(3) Millan, M. J.; Andrieux, A.; Bartzokis, G.; Cadenhead, K.; Dazzan, P.; Fusar-Poli, P.; Gallinat, J.; Giedd, J.; Grayson, D. R.; Heinrichs, M.; *et al.* Altering the Course of Schizophrenia: Progress and Perspectives. *Nat. Rev. Drug Discov.* **2016**, *15*, 485–515.

(4) de Jong, I. E. M.; Mørk, A. Antagonism of the 5-HT6 Receptor – Preclinical Rationale for the Treatment of Alzheimer's Disease. *Neuropharmacology* **2017**, *125*, 50–63.

(5) Vanda, D.; Soural, M.; Canale, V.; Chaumont-Dubel, S.; Satała, G.; Kos, T.; Funk, P.; Fülöpová, V.; Lemrová, B.; Koczurkiewicz, P.; *et al.* Novel Non-Sulfonamide 5-HT_6 receptor Partial Inverse Agonist in a Group of imidazo[4,5-*b*]pyridines with Cognition Enhancing Properties. *Eur. J. Med. Chem.* **2018**, *144*, 716–729.

(6) Ivachtchenko, A. V.; Lavrovsky, Y.; Ivanenkov, Y. A. AVN-211, Novel and Highly Selective 5-HT_6 Receptor Small Molecule Antagonist, for the Treatment of Alzheimer's Disease. *Mol. Pharm.* **2016**, *13* (3), 945–963.

(7) Yun, H.-M.; Kim, S.; Kim, H.-J.; Kostenis, E.; Kim, J. Il; Seong, J. Y.; Baik, J.-H.; Rhim, H. The Novel Cellular Mechanism of Human 5-HT_6 Receptor through an Interaction with Fyn. *J. Biol. Chem.* **2007**, *282* (8), 5496–5505.

(8) Jacobshagen, M.; Niquille, M.; Chaumont-Dubel, S.; Marin, P.; Dayer, A. The Serotonin 6 Receptor Controls Neuronal Migration during Corticogenesis via a Ligand-Independent Cdk5-Dependent Mechanism. *Development* **2014**, *141* (17), 3370–3377.

(9) Duhr, F.; Déléris, P.; Raynaud, F.; Séveno, M.; Morisset-Lopez, S.; Mannoury La Cour, C.; Millan, M. J.; Bockaert, J.; Marin, P.; Chaumont-Dubel, S. Cdk5 Induces Constitutive Activation of 5-HT_6 Receptors to Promote Neurite Growth. *Nat. Chem. Biol.* **2014**, *10* (7), 590–597.

(10) Meffre, J.; Chaumont-Dubel, S.; Mannoury la Cour, C.; Loiseau, F.; Watson, D. J. G.; Dekeyne, A.; Séveno, M.; Rivet, J. M.; Gaven, F.; Déléris, P.; *et al.* 5-HT6 Receptor Recruitment of mTOR as a Mechanism for Perturbed Cognition in Schizophrenia. *EMBO Mol. Med.* **2012**, *4* (10), 1043–1056.

(11) Nadim, W. D.; Chaumont-Dubel, S.; Madouri, F.; Cobret, L.; De Tauzia, M.-L.; Zajdel, P.; Bénédetti, H.; Marin, P.; Morisset-Lopez, S. Physical Interaction between Neurofibromin and Serotonin 5-HT_6 Receptor Promotes Receptor Constitutive Activity. *Proc. Natl. Acad. Sci.* **2016**, *113* (43), 12310–12315.

(12) Dawson, L. A.; Nguyen, H. Q.; Li, P. The 5-HT_6 Receptor Antagonist SB-271046 Selectively Enhances Excitatory Neurotransmission in the Rat Frontal Cortex and Hippocampus. *Neuropsychopharmacology* **2001**, *25* (5), 662–668.

(13) Gérard, C.; Martres, M. P.; Lefèvre, K.; Miquel, M. C.; Vergé, D.; Lanfumey, L.; Doucet, E.; Hamon, M.; El Mestikawy, S. Immune-Localization of Serotonin 5-HT_6 Receptor-like Material in the Rat Central Nervous System. *Brain Res.* **1997**, *746* (1–2), 207–219.

(14) Lacroix, L. P.; Dawson, L. A.; Hagan, J. J.; Heidbreder, C. A. 5-HT_6 Receptor Antagonist SB-271046 Enhances Extracellular Levels of Monoamines in the Rat Medial Prefrontal Cortex. *Synapse* **2004**, *51* (2), 158–164.

(15) Tassone, A.; Madeo, G.; Schirinzi, T.; Vita, D.; Puglisi, F.; Ponterio, G.; Borsini, F.; Pisani, A.; Bonsi, P. Activation of 5-HT_6 Receptors Inhibits Corticostriatal Glutamatergic Transmission. *Neuropharmacology* **2011**, *61* (4), 632–637.

(16) Riemer, C.; Borroni, E.; Levet-Trafit, B.; Martin, J. R.; Poli, S.; Porter, R. H. P.; Bös, M. Influence of the 5-HT_6 Receptor on Acetylcholine Release in the Cortex: Pharmacological Characterization of 4-(2-Bromo-6-Pyrrolidin-1-ylpyridine-4-Sulfonyl)phenylamine, a Potent and Selective 5-HT_6 Receptor Antagonist. *J. Med. Chem.* **2003**, *46* (7), 1273–1276.

(17) Partyka, A.; Jastrzębska-Więsek, M.; Antkiewicz-Michaluk, L.; Michaluk, J.; Wąsik, A.; Canale, V.; Zajdel, P.; Kołaczkowski, M.; Wesołowska, A. Novel Antagonists of 5-HT_6 And/or 5-HT_7 Receptors Affect the Brain Monoamines Metabolism and Enhance the Anti-Immobility Activity of Different Antidepressants in Rats. *Behav. Brain Res.* **2019**, *359*, 9–16.

(18) Chen, P.-C.; Lao, C.-L.; Chen, J.-C. The D3 Dopamine Receptor Inhibits Dopamine Release in PC-12/hD3 Cells by Autoreceptor Signaling via PP-2B, CK1, and Cdk-5. *J. Neurochem.* **2009**, *110* (4), 1180–1190.

(19) Salles, M.-J.; Hervé, D.; Rivet, J.-M.; Longueville, S.; Millan, M. J.; Girault, J.; Cour, C. M. la. Transient and Rapid Activation of Akt/GSK-3β and mTORC1 Signaling by D_3 Dopamine Receptor Stimulation in Dorsal Striatum and Nucleus Accumbens. *J. Neurochem.* **2013**, *125* (4), 532–544.

(20) Millan, M. J.; Di Cara, B.; Dekeyne, A.; Panayi, F.; De Groote, L.; Sicard, D.; Cistarelli, L.; Billiras, R.; Gobert, A. Selective Blockade of Dopamine D_3 versus D_2 Receptors Enhances Frontocortical Cholinergic Transmission and Social Memory in Rats: A Parallel Neurochemical

and Behavioural Analysis. *J. Neurochem.* **2006**, *100* (4), 1047–1061.

(21) Sokoloff, P.; Leriche, L.; Diaz, J.; Louvel, J.; Pumain, R. Direct and Indirect Interactions of the Dopamine D_3 Receptor with Glutamate Pathways: Implications for the Treatment of Schizophrenia. *Naunyn. Schmiedebergs. Arch. Pharmacol.* **2013**, *386* (2), 107–124.

(22) Watson, D. J. G.; Loiseau, F.; Ingallinesi, M.; Millan, M. J.; Marsden, C. A.; Fone, K. C. F. Selective Blockade of Dopamine D_3 Receptors Enhances While D_2 Receptor Antagonism Impairs Social Novelty Discrimination and Novel Object Recognition in Rats: A Key Role for the Prefrontal Cortex. *Neuropsychopharmacology* **2012**, *37* (3), 770–786.

(23) Allen, N. J.; Lyons, D. A. Glia as Architects of Central Nervous System Formation and Function. *Science* **2018**, *362* (6411), 181–185.

(24) Bylicky, M. A.; Mueller, G. P.; Day, R. M. Mechanisms of Endogenous Neuroprotective Effects of Astrocytes in Brain Injury. *Oxid. Med. Cell. Longev.* **2018**, DOI: 10.1155/2018.6501031

(25) Grychowska, K.; Satała, G.; Kos, T.; Partyka, A.; Colacino, E.; Chaumont-Dubel, S.; Bantreil, X.; Wesołowska, A.; Pawłowski, M.; Martinez, J.; *et al.* Novel 1*H*-Pyrrolo[3,2-c]quinoline Based 5-HT_6 Receptor Antagonists with Potential Application for the Treatment of Cognitive Disorders Associated with Alzheimer's Disease. *ACS Chem. Neurosci.* **2016**, *7* (7), 972–983.

(26) González-Vera, J. A.; Medina, R. A.; Martín-Fontecha, M.; Gonzalez, A.; De La Fuente, T.; Vázquez-Villa, H.; García-Cárceles, J.; Botta, J.; McCormick, P. J.; Benhamú, B.; *et al.* A New Serotonin 5-HT_6 Receptor Antagonist with Procognitive Activity - Importance of a Halogen Bond Interaction to Stabilize the Binding. *Sci. Rep.* **2017**, *7*, 1–10.

(27) Grychowska, K.; Kurczab, R.; Śliwa, P.; Satała, G.; Dubiel, K.; Matłoka, M.; Moszczyński-Pętkowski, R.; Pieczykolan, J.; Bojarski, A. J.; Zajdel, P. Pyrroloquinoline Scaffold-Based 5-HT_6R Ligands: Synthesis, Quantum Chemical and Molecular Dynamic Studies, and Influence of Nitrogen Atom Position in the Scaffold on Affinity. *Bioorg. Med. Chem.* **2018**, *26* (12), 3588–3595.

(28) Kurczab, R.; Canale, V.; Satała, G.; Zajdel, P.; Bojarski, A. J. Amino Acid Hot Spots of Halogen Bonding: A Combined Theoretical and Experimental Case Study of the 5-HT_7 Receptor. *J. Med. Chem.* **2018**, *61* (19), 8717–8733.

(29) Drop, M.; Bantreil, X.; Grychowska, K.; Mahoro, G. U.; Colacino, E.; Pawłowski, M.; Martinez, J.; Subra, G.; Zajdel, P.; Lamaty, F. Continuous Flow Ring-Closing Metathesis, an Environmentally-Friendly Route to 2,5-Dihydro-1I-Pyrrole-3-Carboxylates. *Green Chem.* **2017**, *19* (7), 1647–1652.

(30) Haddach, A. A.; Kelleman, A.; M.V., D.-R. An Efficient Method for the *N*-Debenzylation of Aromatic Heterocycles. *Synth. Commun.* **2004**, *34* (17), 3121–3127.

(31) Oscar M. Saavedra, Karila, Dominique Brossard, Anne Rojas, D. D.; Arnaud Gohier, Clotilde Mannoury la Cour, Mark J. Millan, J.-C. O.; Hanessian, S. Design and Synthesis of Novel N-Sulfonyl-2-Indoles That Behave as 5-HT6receptor Ligands with Significant Selectivity for D_3 over D_2 receptors. *Bioorganic Med. Chem.* **2017**, *25* (1), 38–52.

(32) Zajdel, P.; Marciniec, K.; Maślankiewicz, A.; Satała, G.; Duszyńska, B.; Bojarski, A. J.; Partyka, A.; Jastrzębska-Więsek, M.; Wróbel, D.; Wesołowska, A.; *et al.* Quinoline- and Isoquinoline-Sulfonamide Derivatives of LCAP as Potent CNS Multi-receptor—5-HT_{1A}/5-HT_{2A}/5-HT_7 and D_2/D_3/D_4—agents: The Synthesis and Pharmacological Evaluation. *Bioorg. Med. Chem.* **2012**, *20* (4), 1545–1556.

(33) Fabritius, C.-H.; Pesonen, U.; Messinger, J.; Horvath, R.; Salo, H.; Gałęzowski, M.; Galek, M.; Stefańska, K.; Szeremeta-Spisak, J.; Olszak-Płachta, M.; *et al.* 1-Sulfonyl-6-Piperazinyl-7-Azaindoles as Potent and Pseudo-Selective 5-HT_6 Receptor Antagonists. *Bioorg. Med. Chem. Lett.* **2016**, *26* (11), 2610–2615.

(34) Zajdel, P.; Subra, G.; Bojarski, A. J.; Duszyńska, B.; Pawłowski, M.; Martinez, J. Arylpiperazines with *N*-Acylated Amino Acids as 5-HT_{1A} receptor Ligands. *Bioorganic Med. Chem. Lett.* **2006**, *16* (13), 3406–3410.

(35) Kurczab, R.; Śliwa, P.; Rataj, K.; Kafel, R.; Bojarski, A. J. The Salt Bridge in Ligand-Protein Complexes - Systematic Theoretical and Statistical Investigations. *J. Chem. Inf. Model.* **2018**, DOI: 10.1021/acs.jcim.8b00266

(36) Di Malta, C.; Fryer, J. D.; Settembre, C.; Ballabio, A. Astrocyte Dysfunction Triggers Neurodegeneration in a Lysosomal Storage Disorder. *Proc. Natl. Acad. Sci.* **2012**, *109* (35), E2334–E2342.

(37) Kurczab, R.; Ali, W.; Łażewska, D.; Kotańska, M.; Jastrzębska-Więsek, M.; Satała, G.; Więcek, M.; Lubelska, A.; Latacz, G.; Partyka, A.; *et al.* Computer-Aided Studies for Novel Arylhydantoin 1,3,5-Triazine Derivatives as 5-HT_6 Serotonin Receptor Ligands with Antidepressive-Like, Anxiolytic and Antiobesity Action *In Vivo*. *Molecules* **2018**, DOI: 10.3390/molecules23102529.

(38) Łażewska, D.; Kurczab, R.; Więcek, M.; Kamińska, K.; Satała, G.; Jastrzębska-Więsek, M.; Partyka, A.; Bojarski, A. J.; Wesołowska, A.; Kieć-Kononowicz, K.; *et al.* The Computer-Aided Discovery of Novel Family of the 5-HT_6 Serotonin Receptor Ligands among Derivatives of 4-Benzyl-1,3,5-Triazine. *Eur. J. Med. Chem.* **2017**, *135*, 117–124.

(39) Chien, E. Y. T.; Liu, W.; Zhao, Q.; Katritch, V.; Han, G. W.; Hanson, M. A.; Shi, L.;

Newman, A. H.; Javitch, J. A.; Cherezov, V.; *et al.* Structure of the Human Dopamine D_3 Receptor in Complex with a D_2/D_3 Selective Antagonist. *Science* **2010**, *330* (6007), 1091–1095.

(40) Schrodinger Release 2017-3, LigPrep, Schrodinger, LLC, New York, NY, 2017. (41) Schrodinger Release 2017-3, Epik, Schrodinger, LLC, New York, NY, 2017. (42) Harder, E.; Damm, W.; Maple, J.; Wu, C.; Reboul, M.; Xiang, J. Y.; Wang, L.; Lupyan, D.; Dahlgren, M. K.; Knight, J. L.; *et al.* OPLS3 : A Force Field Providing Broad Coverage of Drug-like Small Molecules and Proteins. **2016**, DOI 10.1021/acs.jctc.5b00864

(43) Schrodinger Release 2017-3, Glide, Schrodinger, LLC, New York, NY, 2017.

(44) Schrödinger Release 2017-3: QSite, Schrödinger, LLC, New York, NY, 2017.

(45) Sherman, W.; Day, T.; Jacobson, M. P.; Friesner, R. A.; Farid, R. Novel Procedure for Modeling Ligand/Receptor Induced Fit Effects. *J. Med. Chem.* **2006**, *49* (2), 534–553.

(46) Kooistra, A. J.; Kuhne, S.; de Esch, I. J. P.; Leurs, R.; de Graaf, C. A Structural Chemogenomics Analysis of Aminergic GPCRs: Lessons for Histamine Receptor Ligand Design. *Br. J. Pharmacol.* **2013**, *170* (1), 101–126.

(47) Schrödinger Release 2017-3: QSite, Schrödinger, LLC, New York, NY, 2017.

(48) Murphy, R. B.; Philipp, D. M.; Friesner, R. A. A Mixed Quantum Mechanics/molecular Mechanics (QM/MM) Method for Large-Scale Modeling of Chemistry in Protein Environments. *J. Comput. Chem.* **2000**, *21* (16), 1442–1457.

(49) Schrödinger Release 2017-3 : Desmond Molecular Dynamics System, D. E. Shaw Research, New York, NY, 2017. Maestro-Desmond Interoperability Tools, Schrödinger, New York, NY, 2017 .

(50) Lomize, M. A.; Pogozheva, I. D.; Joo, H.; Mosberg, H. I.; Lomize, A. L. OPM Database and PPM Web Server : Resources for Positioning of Proteins in Membranes. *Nucleic Acids Res.* **2012**, *40*, 370–376.

(51) Bojarski, A. J.; Cegla, M. T.; Charakchieva-Minol, S.; Mokrosz, M. J.; Mackowiak, M.; Misztal, S.; Mokrosz, J. L. Structure-Activity Relationship Studies of CNS Agents. Part 9: 5-HT_{1A} and 5-HT_2 Receptor Affinity of Some 2- and 3-Substituted 1,2,3,4-Tetrahydro-Beta-Carbolines. *Pharmazie* **1993**, *48* (4), 289–294.

(52) Paluchowska, M. H.; Bugno, R.; Duszyńska, B.; Tatarczyńska, E.; Nikiforuk, A.; Lenda, T.; Chojnacka-Wójcik, E. The Influence of Modifications in Imide Fragment Structure on 5-HT_{1A} and 5-HT_7 Receptor Affinity and in Vivo Pharmacological Properties of Some New 1-(M-Trifluoromethylphenyl)piperazines. *Bioorg. Med. Chem.* **2007**, *15* (22), 7116–7125.

(53) Cheng, Y.; Prusoff, W. H. Relationship between the Inhibition Constant (Ki) and the Concentration of Inhibitor Which Causes 50% Inhibition (I50) of an Enzymatic Reaction.

Biochem. Pharmacol. **1973**, *22*, 3099–3108.

(54) López, S.; Martá, M.; Sequeda, L. G.; Celis, C.; Sutachan, J. J.; Albarracín, S. L. Cytoprotective Action against Oxidative Stress in Astrocytes and Neurons by Bactris Guineensis (L.) H.E. Moore (Corozo) Fruit Extracts. *Food Chem. Toxicol.* **2017**, *109*, 1010–1017.

(55) Kolla, N.; Wei, Z.; Richardson, J. S.; Li, X.-M. Amitriptyline and Fluoxetine Protect PC12 Cells from Cell Death Induced by Hydrogen Peroxide. *J. Psychiatry Neurosci.* **2005**, *30* (3), 196–201.

(56) Olatunji, O. J.; Chen, H.; Zhou, Y. Neuroprotective Effect of Trans-N-Caffeoyltyramine from Lycium Chinense against H_2O_2 Induced Cytotoxicity in PC12 Cells by Attenuating Oxidative Stress. *Biomed. Pharmacother.* **2017**, *93*, 895–902.

(57) Cheruku, S. P.; Ramalingayya, G. V.; Chamallamudi, M. R.; Biswas, S.; Nandakumar, K.; Nampoothiri, M.; Gourishetti, K.; Kumar, N. Catechin Ameliorates Doxorubicin-Induced Neuronal Cytotoxicity in *in Vitro* and Episodic Memory Deficit in *in Vivo* in Wistar Rats. *Cytotechnology* **2018**, *70* (1), 245–259.

(58) Popik, P.; Holuj, M.; Nikiforuk, A.; Kos, T.; Trullas, R.; Skolnick, P. 1-Aminocyclopropanecarboxylic Acid (ACPC) Produces Procognitive but Not Antipsychotic-like Effects in Rats. *Psychopharmacology (Berl).* **2015**, *232* (6), 1025–1038.

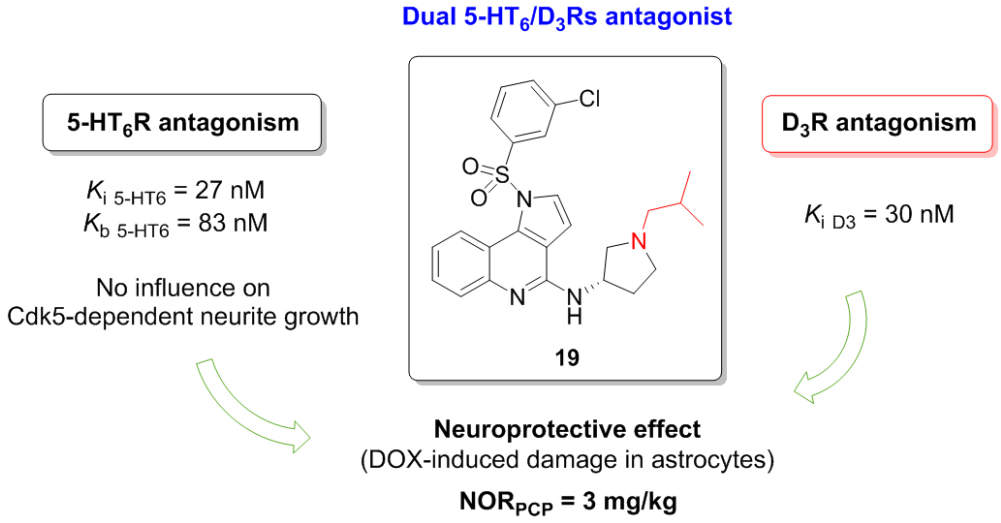

273x143mm (96 x 96 DPI)